Egypt. J. Chem. **Vol. 67,** No. 11 pp. 131 - 153 (2024)

Egyptian Journal of Chemistry

http://ejchem.journals.ekb.eg/

Nanocarrier-Based Formulation and Encapsulation of Imidacloprid: Design and Toxicological Assessment on *Spodoptera littoralis* Larvae Using Chitosan-Dextran Sulfate

Mostafa Hosny[1], El-Sayed H. Shaurub[1], Hesham A. Yousef[1*], Heba M. Fahmy[2]

1. *Entomology Department, Faculty of Science, Cairo University, Giza, Egypt*
2. *Biophysics Department, Faculty of Science, Cairo University, Giza, Egypt*

Abstract

The cotton leafworm, *Spodoptera littoralis*, is a voracious pest that poses significant agricultural challenges. Traditional pesticide applications have not only fostered resistance in *S. littoralis* but also have had detrimental environmental impacts. Nanotechnology offers a promising alternative through nano-pesticide formulations. The controlled-release (CR) nanoformulations of the neonicotinoid imidacloprid were characterized by various spectroscopic techniques, including transmission and scanning electron microscopy, atomic force microscopy, and Fourier transform infrared spectroscopy. Toxicological and biochemical impacts of standard and CR neonicotinoid imidacloprid nanoformulation, encapsulated with chitosan-dextran sulfate (CS-DS) on 4th-instar larvae of *S. littoralis* were evaluated. Our findings indicate that both the unencapsulated and CS-DS encapsulated imidacloprid nanoparticles (NPs) exhibit increased toxicity over time, with the encapsulated form showing the highest lethality. Bioaccumulation of imidacloprid was most pronounced in the insect gut, followed by the brain and hemolymph. Exposure to both forms of imidacloprid resulted in a significant reduction in energy reserve levels, as well as decreased glutathione and acetylcholinesterase activity in the surviving larvae. Conversely, markers of oxidative stress were significantly elevated. Notably, these effects were more pronounced with the imidacloprid-loaded CS-DS NPs than with the unencapsulated pesticide. Our research suggests that CR nanoformulations of imidacloprid may mitigate the development of resistance in *S. littoralis* by reducing the quantity of pesticide reaching the target site, thereby offering a more sustainable pest management strategy.

*Keywords***:** Nano-imidacloprid; Chitosan-dextran; Toxicological bioassays; Oxidative status; Antioxidant enzymes; Detoxification enzymes.

I. Introduction

Nanotechnology is a new promising field greatly used to solve many problems in different applied sciences, such as medicine, biology, agriculture, pharmaceuticals, and genetic engineering, to make the life easier.

The Egyptian cotton leafworm, *Spodoptera littoralis* (Boisduval) (Lepidoptera: Noctuidae), poses a significant threat not just to cotton harvests but also to several other economic crops and vegetables [1]. About 120 plant species belonging to 44 families have been documented as hosts [2]. This pest exhibits a wide geographical distribution, involving the Asian continent, the Middle East, the entire Mediterranean region, and the north of Africa [2].

The neonicotinoid insecticide imidacloprid is a systemic insecticide in the chloronicotinyl class. It is among the neonicotinoids that have the greatest sales worldwide [3,4], targeting nicotinic acetylcholine receptors, resulting in Na+ entry increase and K+ exit, blocking the postsynaptic receptors irreversibly, causing convulsions and paralysis, and eventually killing the insect [4]. Since its first identification, imidacloprid has gained significant popularity in controlling diverse plant-feeding pests that engage in sucking behavior [5]. However, one of the most promising and successful pesticides for controlling lepidopteran pests is imidacloprid [6,7]. Besides, It is an essential component of integrated pest management (IPM) in addition to the integrated risk management (IRM) systems [8] due to its reduced toxicity to animals [9]. Nevertheless, imidacloprid causes toxicity to pollinators, including honeybees and crustaceans [4,10].

Over the past 20 years, the attention to controlled-release technology has increased since only 0.1% of pesticides reach their intended targets,

*Corresponding author e-mail: heshamyousef@sci.cu.edu.eg.; (Hesham A. Yousef (HY);
Received: 13 April 2024, Revised: 27 May 2024, Accepted: 30 May 2024
DOI: 10.21608/EJCHEM.2024.282101.9588

necessitating their repeated application, which ultimately results in several environmental hazards [11,12]. This technology would facilitate more convenient storage and distribution processes and improve the duration of pesticide effectiveness beyond its initial application [13]. The use of nanotechnologies in dealing with insect pests is commonly recognized as an ecologically benign and highly successful solution for insect management in green agriculture [14]. Due to the significant toxicity of imidacloprid [10,15], controlled release and ongoing monitoring are essential.

Chitosan (CS) is a naturally occurring, safe, and inexpensive byproduct of chitin deacetylation. It is an environmentally friendly, biodegradable, antimicrobial, non-hazardous, and absorbing material. Chitosan binds strongly to the epidermis layer of both stems and leaves, prolonging the interaction duration and facilitating the absorption of bioactive compounds [16]. Chen et al. [17] have successfully developed a novel CS nanoparticle (NP) class that utilizes dextran sulfate (DS) as a polyanionic polymer to improve stability and achieve controlled release of various chemicals. One of the primary advantages of encasing agrochemicals in chitosan is its ability to function as a protective reservoir for active components from the outside world while they are in the chitosan domain and then manage their release [15,18]. Additionally, the list of active chemicals that can be used in minimum-risk pesticide products without having to register or comply with other Federal Insecticide Program standards now includes chitosan (poly-D-glucosamine) [19].

The process of oxidative metabolism within cells represents the continuous production of reactive oxygen species (ROS). Ilhan et al. [20] have observed that ROS exhibits typical functionality in physiological cellular processes when present in low to moderate concentrations. Although normal cellular metabolic processes produce reactive oxygen species (ROS), applying pesticides to control certain insects causes an imbalance in the generation of ROS. Insecticides may cause the production of ROS, a rise in oxidative stress, and an increase in the antioxidants superoxide dismutase (SOD) and reduced glutathione (GSH) [21]. Moreover, the involvement of various detoxification enzymes, e.g., glutathione S-transferase (GST) and acetylcholinesterase (AChE), in the metabolism of multiple xenobiotics have been reported [22,23].

The indiscriminate and widespread use of pesticides for *S. littoralis* management has led to the development of resistance. Moreover, extensive use of pesticide application has also led to negative impacts on the environment [12,24].Hence, an ecological pest management system that is environmentally friendly and sustainable must be established. In this scenario, we hypothesized that controlled release could reduce the risk of harmful effects on the environment caused by excessive chemical exposure required for effective pest management [13,25].

In this study, the 4th instar larvae of *S. Littoralis* were chosen based on its higher effectiveness among larval instars causing the agriculture crops damage [7]. The current study aimed to (i) synthesize the controlled-release nanoformulations of imidacloprid by adding imidacloprid to a CS-DS formulation using encapsulation technique and characterization, producing imidacloprid-loaded CS-DS NPs, (ii) evaluate the toxicity of unloaded imidacloprid and imidacloprid-loaded CS-DS NPs against 4th-instar larvae of *S. littoralis*, (iii) identifying the concentrations of imidacloprid in the different body organs (gut, hemolymph, and brain) due to treatments with unloaded imidacloprid and imidacloprid-loaded CS-DS NPs, and (iv) quantifying the levels of oxidative stress markers (malondialdehyde, and GSH), antioxidant enzymes (SOD, ascorbate peroxidase, APOX, and catalase, CAT), detoxification enzymes (AChE and GST), and nitric oxide (NO) against 4th-instar larvae of *S. littoralis*.

2. Material and Methods

2.1. Insects

The stock cultivation of *S. littoralis* was taken from a colony that had been raised without pesticides for several generations at the Plant Protection Institute, Giza, Egypt. Adults were fed a 10% sucrose solution, while larvae were given fresh castor bean leaves (*Ricinus communis* L.). Insects were kept at 25 ± 2°C, 75 ± 5% relative humidity, and a 12-hour light: 12-hour dark photoperiod.

2.2. Chemicals

Chitosan (CS) (deacetylation 96%), dextran sulfate sodium salt (DS) and sodium hydroxide (Applichem and Sigma Aldrich, Germany), glacial acetic acid (g.a.a.) (99.7%) (PioChem for Egypt's chemicals), 1-(6-chloro-3-pyridylmethyl)-N-notroimidazolidin-2-ylideneamine (imidacloprid, 35% SC) (SUN-DAT, Singapore), and hydrochloric acid (SDFCL, India).

2.3. Preparation methods

2.3.1. Chitosan-dextran sulfate nanocarrier preparation

The chitosan-dextran sulfate nanoparticles (CS-DS NPs) were synthesized using a refined complex coacervation technique, building upon the foundational method described by Chen et al. [26]. Initially, chitosan was prepared by dissolving 0.1 g of high molecular weight chitosan (85% deacetylation) in 100 ml of 1% (v/v) glacial acetic acid. This

solution was then subjected to magnetic stirring at 600 rpm for 24 hours to ensure complete dissolution and homogeneity. Concurrently, 0.1% (w/v) dextran sulfate (DS) solution was prepared by dissolving 0.1 g of DS (molecular weight 5000-7000 kDa) in 100 ml of deionized water at room temperature, with gentle stirring.

The coacervation process was initiated by the gradual addition of 50 ml of the DS solution to the chitosan solution under constant stirring at 800 rpm. This dropwise addition was conducted over a period of 30 minutes to ensure controlled interaction between the positively charged chitosan and the negatively charged DS, leading to the formation of stable nanoparticles. The resultant mixture was then left to stir for an additional 2 hours to stabilize the nanoparticle formation. Then, the nanoparticles were isolated by centrifugation at 10,000 g for 15 minutes. The supernatant was discarded, and the nanoparticle pellet was washed thrice with deionized water to remove any unreacted materials.

2.3.2. Imidacloprid loading of the prepared chitosan-dextran sulfate nanocarrier

The procedure for loading imidacloprid onto the prepared CS-DS NPs was meticulously optimized to enhance loading efficiency. A 0.1% (w/v) chitosan solution was prepared as described in section 2.3.1, with the pH adjusted to 5.5 using 0.1 M hydrochloric acid to promote imidacloprid binding. An imidacloprid solution was prepared at a concentration of 0.5 mg/ml in deionized water, and the pH was adjusted to 7.0 using 0.1 M sodium hydroxide to ensure the drug's stability and solubility. A 0.1% (w/v) DS solution was also prepared, with the pH adjusted to 7.0 to match that of the imidacloprid solution.

The loading process commenced with the simultaneous and gradual addition of 50 ml of the imidacloprid solution and 50 ml of the DS solution to 75 ml of the chitosan solution, drop by drop while stirring at 800 rpm. This was done over 30 minutes to facilitate the encapsulation of imidacloprid within the nanoparticles. The mixture was then stirred for an additional 2 hours to ensure maximum loading. The loaded nanoparticles were then separated by centrifugation at 10,000 g for 20 minutes. The supernatant was removed, and the pellet was washed with deionized water to eliminate any free imidacloprid. The loading efficiency was quantified by measuring the concentration of imidacloprid in the supernatant using high-performance liquid chromatography (HPLC), as per the methods described by Cui et al. [27] and Fathy et al. [28].

2.4. Characterization of the prepared nanoformulations

2.4.1. Transmission electron microscopy

Transmission electron microscopy (TEM) was used to determine the size, shape, and magnification of the formulated CS-DS NPs and the imidacloprid-loaded CS-DS NPs. Subsequently, every diluted solution was carefully deposited onto a copper grid and desiccated for 15 min. Negative staining was done on the two samples by applying a 1% phosphotungstic acid solution and air-dried for about one sec. After that, the photographs were captured with a high-resolution TEM (Jeol JEM 1230, Tokyo, Japan) [28].

2.4.2. Scanning electron microscopy and energy-dispersive X-ray spectrometer

Scanning electron microscopy (SEM) (Quanta TM 250 FEG, USA) technique was employed to analyze the surface structure and quantify the CS-DS NPs and imidacloprid-loaded CS-DS nanoparticles. Additionally, an energy-dispersive X-ray imaging spectrometer (EDX) was used to determine the concentrations of elements in the formulations. The voltage used was 20 KV.

2.4.3. Particle size and zeta potential

Malvern Instruments' Zetasizer Nano ZS90 instrument was used to analyze the potential zeta and size distribution profile of CS-DS NPs and imidacloprid-loaded CS-DS NPs at 25°C using dynamic light scattering (DLS). Deionized water was used to dilute the formulations before testing. After particle size measurement, the zeta potential was calculated at 1.33 refractive index and 0.89 cp viscosity. Each sample had three analyses to derive mean values and standard errors.

2.4.4. Atomic force microscopy

A well-resolved, without-contact atomic force microscope (Wet – SPM9600, Shimadzu, Japan) evaluated CS-DS NPs and imidacloprid-loaded CS-DS NPs for topographic and mechanical properties. The cantilever's tip was scanned on the sample's surface using non-contact atomic force microscopy (AFM). At 10–100 Å, this point did not touch the sample. Thus, scanning does not disturb or damage the sample. The attraction forces between the tip and the sample were used to quantify the surface texture and its topography using non-contact AFM.

2.4.5. X-ray diffraction spectra

Dry samples of CS-DS NPs and imidacloprid-loaded CS-DS NPs should be ready before estimation, testing, and processing using a basic planetary ball factory (LZQM0.4L, Shicheng Desert Spring Mineral Gear Assembling Co., Ltd.), in which a ball factory of treated steel of 0.1 cm width was put in processing measure with tests for one h at 1500 rpm. Then, the chemical composition and the crystalline phase were determined using an X-ray diffractometer (XRD, D8-Discover, Bruker, Cu Kα radiation (1.5418 Å), Madison, WI, USA) working

with a voltage of 40 kV, current of 40 mA, and a step filter of 0.01°.

2.4.6. Fourier transform infrared spectroscopy

The Fourier transform infrared **(**FTIR) spectrometer (Edwards High Vacuum, Craeley, Sussex, England) was used to examine how imidacloprid interacted with the surface of CS-DS NPs. This assessment was conducted for the pellet of CS-DS NPs and imidacloprid-loaded CS-DS NPs. The scanning speed of the FTIR spectroscopy was 2 mm per second, while the spectral resolution achieved was 4 cm^{-1}. The observed spectrum patterns were documented due to the relationship between wave number and transmittance percentage.

2.4.7. Raman spectroscopy

Non-destructive chemical examination of chemical structure, phase, crystal structure, and polymorphism effectively with the interaction between molecules is possible with Raman spectroscopy. The Raman spectra were collected with a Horiba Lab RAM HR evolution spectrometer (Lyon by HORIBA Company, France SAS) equipped with a 532 nm edge laser line, diffraction (450–850 nm), 10% ND filter, 15-second collection period, four collections without a spike filtering process, and an X100 magnification.

2.4.8. In vitro drug release

The release profile of imidacloprid from imidacloprid-loaded CS-DS NPs was studied using the dialysis bag method [29]. The dialysis bags (Sigma-Aldrich) used had a molecular weight cutoff (MWCO) of 12,000 g/mol. To verify imidacloprid sustainability and controlled release in a simulated gastrointestinal system (GIT) environment comparable to that of S. littoralis, studies were performed at a pH value of 10. A 20-ml phosphate-buffered saline (pH 10) solution was produced at 37oC. This solution was administered into every falcon tube in preparation for the laboratory release test. The dialysis bags were filled with equal quantities (5 ml) of each formulation before being immersed in a buffer solution (pH 10) with a volume of 20 ml. To evaluate the amount of imidacloprid released, a 2 ml sample was removed from each formulation buffer tube solution during a specific time frame. These samples were then replaced with fresh buffers. A UV-visible spectrophotometer was used to measure the amounts of released imidacloprid in the samples at 269 nm [28].

2.4.9. High-performance liquid chromatography encapsulation

To determine the encapsulation efficiency of imidacloprid within the CS-DS NPs and to address the solubility concerns of imidacloprid in aqueous environments, the following methodology [28] was employed:

Post-preparation, the imidacloprid-loaded CS-DS NP suspension was centrifuged at 10,000 RPM for 20 minutes using a high-speed centrifuge (VS-18000M, Korea, 220 V/50 HZ power). The supernatant was carefully collected to analyze the unencapsulated, free imidacloprid. High-performance liquid chromatography (HPLC) (Young Lin model 9100 Instrument, Korea) was utilized for this analysis. The chromatographic separation was achieved using a C18 column (250 mm × 4.6 mm × 5 µm). An injection volume of 20 µL was employed, with a constant flow rate of 1.0 ml/min. The detection of imidacloprid was conducted at a UV wavelength of 270 nm. The mobile phase consisted of acetonitrile (ACN) and deionized water in a ratio of 90:10, which was optimized to ensure the complete solubility of imidacloprid, thereby preventing any potential precipitation during the analysis. The total run time for the drug analysis was approximately 9 minutes, with a retention time (RT) for imidacloprid of 3.167 minutes.

The encapsulation efficiency (EE%) was calculated using the following equation, which takes into account the total amount of drug used in the formulation process (Total Drug) and the amount of drug present in the supernatant after separation of the nanoparticles (Free Drug):

Encapsulation Efficiency (EE%) = [(Total Drug - Free Drug) / Total Drug] × 100

This calculation provides an accurate representation of the encapsulation efficiency by considering the initial total amount of imidacloprid used in the formulation. The Total Drug represents the initial amount of imidacloprid intended for encapsulation, and the Free Drug quantified in the supernatant represents the fraction of the drug that did not get encapsulated within the nanoparticles.

2.5. Toxicological bioassays

Thirteen aqueous concentrations of imidacloprid and imidacloprid-loaded CS-DS NPs were prepared (150, 200, 250, 300, 350, 400, 450, 500, 550, 600, 650, 700, and 800 mg/L). Castor-bean leaves, *Ricinus communis L* were separately dipped in each concentration for 45 sec and then air-dried at room temperature [30]. Newly molted 4^{th}-instar larvae of *S. littoralis* were starved overnight [31] and then fed treated leaves for 24, 48, 72, and 120 h. Treated leaves were then replaced by fresh untreated leaves until larvae either died or reached the pre-pupal stage. Castor bean leaves dipped in distilled water and those dipped in CS-DS NPs served as the controls for unloaded imidacloprid and imidacloprid-loaded CS-DS NPs, respectively. Three replications with 20 larvae each (total of 60 larvae) of each concentration and the control were performed. Using

Abbott's calculation formula, percentage mortality was determined and corrected [32]. Using IBM SPSS Statistics Analysis Version 26 and probit analysis [33], the LC_{50} at each time of treatment was estimated. Finally, toxicity index is calculated according to the equation of Sun [34].

2.6. Biochemical assays

2.6.1. Sample preparation

After five days of treatment of 4th-instar larvae with the LC_{50} of unloaded imidacloprid and imidacloprid-loaded CS-DS NPs, the survivors were collected. From each treatment, 0.5g of larval tissue was homogenized on ice in 5 ml of potassium phosphate buffer (0.1 M, pH 7.2), then centrifuged at 8000 rpm for 15 min under cooling (4°C). The supernatant that resulted was obtained and kept at -80°C for further studies [30]. Each treatment was replicated three times. A parallel control was also run and repeated three times.

After dissection, three main parts (brain, gut, and hemolymph) of the surviving larvae were removed. Into three labeled test tubes for each treatment of unloaded imidacloprid and imidacloprid-loaded CS-DS NPs, 0.5g of brain and gut tissues, and 0.5 ml of hemolymph were homogenized on ice in 5 ml of potassium phosphate buffer (0.1 M, pH 7.2), then centrifuged at 8000 rpm for 15 min at 4ºC. The supernatant of each sample was separately collected to quantify imidacloprid and imidacloprid-loaded CS-DS NP concentrations in the three anatomical tissues using the HPLC method.

2.6.2. Determination of total contents of energy reserves

The total protein concentration was determined using the Bradford [35] technique. Coomassie brilliant blue (G-250) dye reagent and standardized bovine serum albumin (BSA) were employed. A UV/Vis Jenway-7305 spectrophotometer (Bibby Scientific Limited, Staffordshire, UK) was used to quantify protein at 595 nm.

The carbohydrate content was determined using the Singh and Sinha [36] technique with an anthrone reagent and glucose as a reference. At 620 nm, the total carbohydrate content was determined.

The phosphovanillin method described by Barnes and Blackstock [37], which used cholesterol as a standard, was followed to determine the total lipid content. Total lipid content was measured at 540 nm.

2.6.3. Oxidative stress markers assays

To determine MDA level as a lipid peroxidation marker, 1.0 ml of supernatant was mixed with 2.0 ml of a solution of 15% (w/v) of trichloroacetic acid (TCA) and 0.375% (w/v) of thiobarbituric acid (TBA) prepared in 0.25 N HCI (pH 3.4). The resulting mixture was boiled in a boiling water bath for 15 minutes before cooling and centrifuged at 1500 × g to separate the resulting precipitate from the tissue sample. The pink color was measured at 532 nm [38].

GSH content was measured using the method of Beutler et al. [39] based on the reaction of GSH with DTNB (5, 5′-dithiobis, 2-nitrobenzoic acid), producing oxidized glutathione (GSSG) and 5-thio-2-nitrobenzoic acid (TNB). TNB content was determined spectrophotometrically at 412 nm. The GSH content was calculated using the GSH standard curve and represented as µg /mg protein.

2.6.4. Antioxidant enzyme assays

The CAT activity was evaluated in conformity with the Aebi [40] approach. 3060 µL of a potassium phosphate buffer (50 mM, pH 7.2), 510 µL of the supernatant, and 40 µL of freshly prepared H_2O_2 (10 mM). At 420 nm, the absorbance was measured.

According to the Misra and Fridovich [41] method, the measurement of SOD activity was determined. The reaction mixture consisted of 87 µL of the supernatant, 35 µL (10 mM) of EDTA, 402 µL (200 mM; pH 10.0) of a sodium carbonate buffer, and 2835 µL (15 mM) of recently developed epinephrine. The absorbance was measured at 480 nm.

Asada [42] determined the activity of ascorbate peroxidase (APOX). The reaction mixture contained 3 mL of phosphate buffer (100 mM, pH 7.2), 0.1 mM EDTA, 0.3 mM ascorbic acid, 0.06 mM H_2O_2, and 0.1 mL of each sample tissue's supernatant. At 290 nm, the absorbance of the sample and blank versus distilled water was measured.

2.6.5. Detoxification enzyme assays

Acetylcholine esterase (AChE) activity was assayed based on the method proposed by Simpson et al. [43] using acetylcholine bromide (ACh Br) as a substrate. The reduction in ACh Br caused by AChE degradation was measured through spectroscopy at 515 nm.

GST activity was determined according to the method of Habig et al. [44] using 1-chloro-2,4-dinitrobenzene) (CDNB) as a substrate. The change in absorbance was measured at 340 nm at a min interval.

2.6.6 Nitric oxide assays

NO activity was determined according to Montgomery and Dymock [45]. The reaction mixture consisted of 0.1 ml of sample, sulphanilamide (10 mmol/L), N-(1-naphthyl)-ethylenediamine (NEDA) (1 mmol/ L), and 0.1 ml of sodium nitrite (50 µmol/L). The absorbance was measured at 540 nm.

The activities of all enzymes were presented in optical density (OD) units as OD/min/mg protein

and all measurements were done in 3 replicates, with a group of 10 insects each.

2.7. Statistical analysis

All data sets were first analyzed for the normality test based on the Shapiro-Wilk test. Data were then presented as the mean ± standard error (SE) for analysis. One-way ANOVA followed by post hoc Tukey's test for multiple comparisons was used to compare group means. Student's *t*-test was carried out to compare the concentrations of unloaded imidacloprid and imidacloprid-loaded CS-Ds NPs in the brain, hemolymph, gut, and whole body. A $P \leq 0.05$ was considered significant for all tests. All statistical calculations were conducted using IBM-SPSS Statistics v.26 (IBM, Armonk, New York, USA).

3. Results

3.1. Characterization of the prepared nanoformulations physically

3.1.1. Transmission electron micrographs

Transmission electron micrographs of CS-DS NPs and imidacloprid-loaded CS-DS NPs are shown in **Fig. 1 A & B**. It successfully showed the formation of homogeneous CS-DS NPs and imidacloprid-loaded CS-DS NPs. The main shapes of the two nanoformulations were virtually spherical, with small aggregations. The thick layer of CS-DS NPs (arrow indicated) visible in the TEM image **(Fig. 1B)** demonstrated that imidacloprid-loaded CS-DS NPs had successfully formed. The average nano-size for the two produced formulations was 74.90 ± 7.3 nm for the CS-DS NPs and 97.42 ± 7.86 nm for imidacloprid-loaded CS-DS NPs.

3.1.2. Scanning electron micrographs

Fig. 2 illustrates SEM images of CS-DS NPs and imidacloprid-loaded CS-DS NPs. For CS-DS NPs, SEM images showed a nearly coherent structure where the surface's CS character predominates **(Fig. 2A)**; imidacloprid-loaded CS-DS NPs, on the other hand, exhibited a compact exterior, with two transparent phases and a porous structure **(Fig. 2B)**.

3.1.3. Energy dispersive X-ray spectroscopy

The main components of the synthesized CS-DS NPs and imidacloprid-loaded CS-DS NPs were identified using the EDX spectrum **(Fig. 3 A & B)**. For CS-DS NPs **(Fig. 3 A)**, the absorption peaks at (0.2, 0.3, 0.5, and 2.3 keV) for carbon, nitrogen, oxygen, and sulfur, respectively, indicate the prominent elements composing CS-DS NPs. For imidacloprid-loaded CS-DS NPs, the spectrum is nearly like that of CS-DS NPs. Still, it's observed that the absorption peak is at 2.4 keV for the chloride element found in imidacloprid (Fig. 3 B), and other small peaks are found for solvent elements of imidacloprid.

3.1.4. Dynamic light scattering

The results of particle size measured by DLS for CS-DS NPs and imidacloprid-loaded CS-DS NPs are shown in **Fig. 4.** The results showed that the mean hydrodynamic diameter of imidacloprid-loaded CS-DS NPs is 164 ± 4.29 nm; larger than that of CS-DS NPs (142 ± 4.24 nm).

3.1.5. Zeta Potential Measurement

CS-DS NPs recorded an average zeta potential of 30.28 ± 3.35 mV, while imidacloprid-loaded CS-DS NPs had a zeta potential of 20.70 ± 3.59 mV.

3.1.6. Atomic force micrograph

Topographic scans of imidacloprid, CS-DS NPs, and imidacloprid-loaded CS-DS NPs produced by AFM are shown in **Fig. 5 A, B, and C,** respectively. The three formulations' nanoscale characteristics, which depict the roughness of their materials, may be seen. The mean roughness values of imidacloprid (1.217±0.296 nm) and imidacloprid-loaded CS-DS NPs were 1.42±0.53 nm, which were greater than those of CS-DS NPs (1.175±0.315 nm).

3.1.7. X-ray diffraction spectra

X-ray powder diffraction is used to analyze the phase identification of CS-DS NPs and imidacloprid-loaded CS-DS NPs. For an average bulk composition, the particles are finely ground and homogenized. As the sample and detector rotate through their respective angles, the intensity of diffracted X-rays is continually recorded. As shown in **Fig. 6,** the powder XRD patterns showed a prominent diffraction peak at an angle of $2\theta = 22.44^{o}$ for CS-DS NPs and 23.54^{o} for imidacloprid-loaded CS-DS NPs.

3.1.8. Fourier transform infrared spectroscopy

FTIR analysis was used to evaluate the crosslinking of CS and DS to generate CS-DS NPs, as well as the interaction of the imidacloprid molecule with these nanoparticles. FTIR spectra of CS-DS NPs and imidacloprid-loaded CS-DS NPs are shown in **Fig. 7.** For the CS-DS NPs spectrum, it was found that type I amine beak at 1639 cm^{-1}. The asymmetric stretch of S=O beak at 1236 cm^{-1} and a strong peak was observed at about 3400 cm^{-1}, characteristic of O–H stretching and intramolecular hydrogen bonds. Two small adjacent bands appeared in the spectrum of polysaccharides. They were noticed at 2857 and 2922 cm^{-1}, corresponding to the C-H symmetric and asymmetric stretching, respectively, and tiny adjacent peaks were recorded at 637, 603, and 1122, which correspond to SO_4 asymmetric bending, S–O–S vibration and C-O stretching, respectively. The FTIR spectrum of imidacloprid-coated CS-DS NPs is nearly similar to

that of CS-DS NPs. Still, it's observed that the overall expansion of the peaks in the range of 3400 cm^{-1} explains the hydrogen bonding between CS-DS NPs and the drug molecule.

3.1.9. Drug encapsulation efficiency

Using HPLC, the drug encapsulation efficiency of imidacloprid-loaded CS-DS NPs prepared at pH 7.4 was 67.824%.

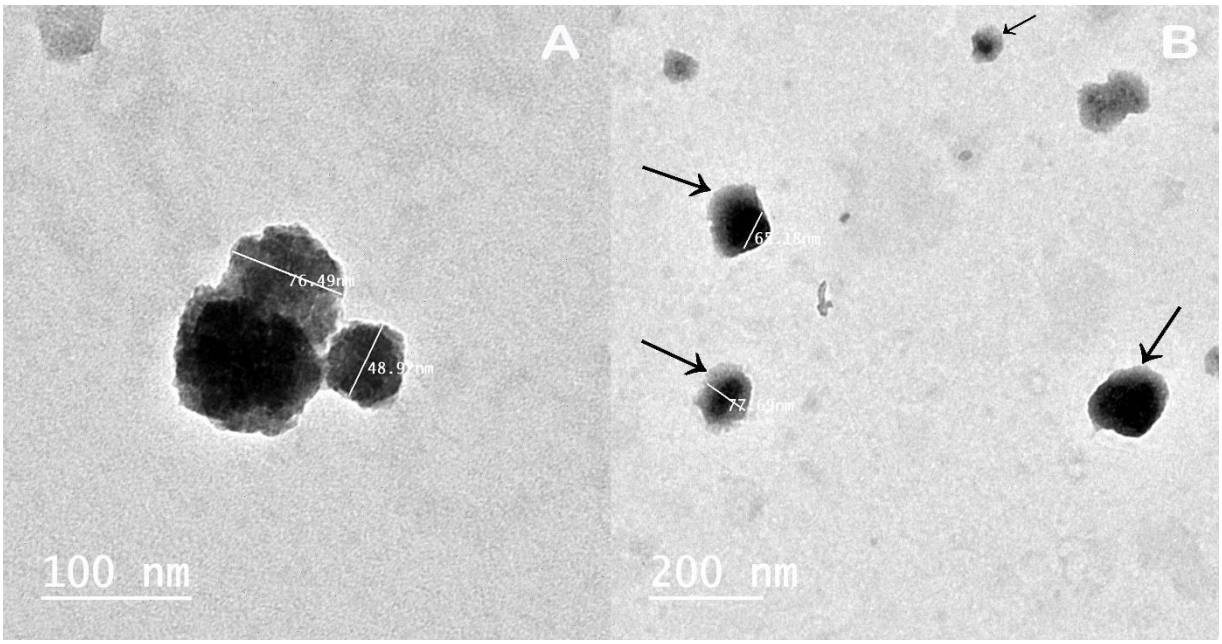

Fig. 1. TEM images for (A) CS-DS NPs and (B) imidacloprid-loaded CS-DS NPs

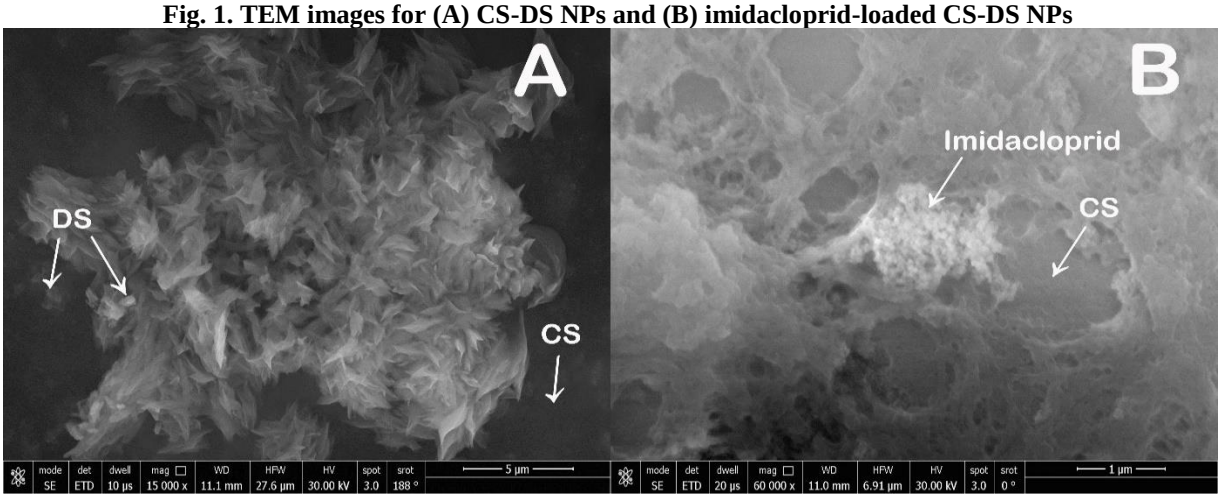

Fig. 2. SEM images of (A) CS- DS NPs and (B) imidacloprid-loaded CS-DS NPs

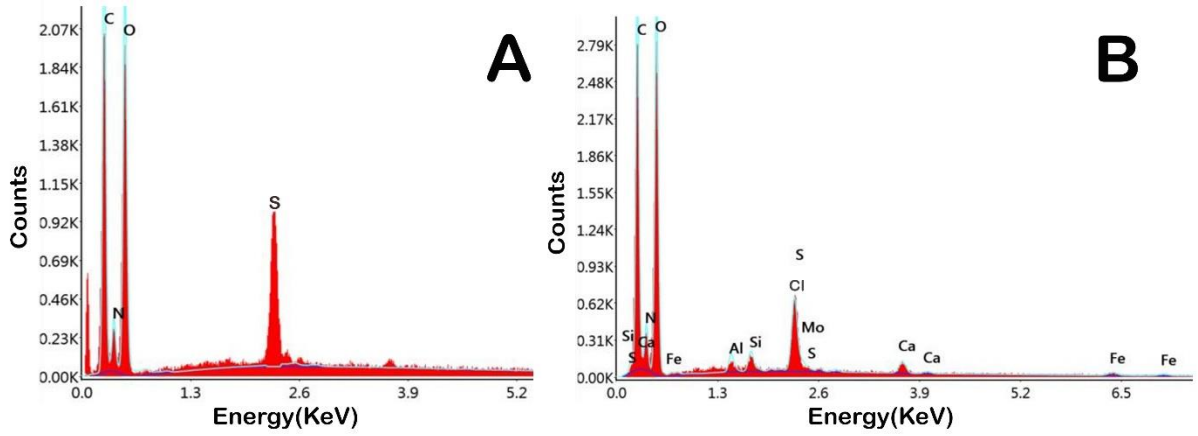

Fig. 3. EDX spectra for (A) CS- DS NPs and (B) imidacloprid-loaded CS-DS NPs

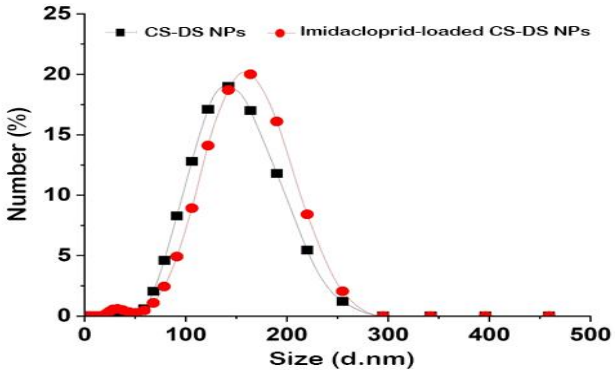

Fig. 4. Particle size distribution for CS-DS NPs and imidacloprid-loaded CS-DS NPs

3.1.10. Raman spectroscopy

Raman spectra of CS-DS NPs and imidacloprid-loaded CS-D NPs are shown in **Fig. 8.** For the CS-DS NPs spectrum, it was found that stretching peaks of CH_3 at 2974 and 2951 cm^{-1} and a stretching peak of CH_2 and CH at 2810 and 2770 cm^{-1}, respectively.

At 1586 $cm^{-1,}$ a stretching band of CO, and at 1557 $cm^{-1,}$ in-plane bending vibrations of NH_2 and bands at 859 and 925 cm^{-1} occurred due to C-O-C stretching. The band at 1359 cm^{-1} is a stretching CH in CH_2OH as a result of hydrogen bonding interactions between CS and DS. The hydrogen-bond network between CS and DS facilitated the highly proton-conductive property of the CS–DS matrix. The Raman spectrum of imidacloprid-loaded CS-DS NPs is virtually identical to that of CS-DS NPs. However, it has been found that peak in-plane bending vibrations at 1578 cm^{-1} of C-H. Stretching beaks of C-N at 1345, 1330, and 994 cm^{-1}. The stretching beak of N-N at 1253 cm^{-1} and N-C-N bond out-of-plane vibration at 350 cm^{-1} and peak at 1447 cm^{-1} indicates hydrogen bonding between CS-DS NPs and the imidacloprid molecule.

3.1.11. In vitro drug release

The in vitro release profile of imidacloprid from the CS-DS nanocarrier was rigorously assessed to evaluate the effectiveness of our nanoformulation. Cumulative release percentages over time were recorded to express the release kinetics of imidacloprid, as depicted in Fig. 9. The release behavior of the unloaded imidacloprid formulation in deionized water was characterized by a burst release pattern, with approximately 90% of the drug being rapidly released within the first 5 hours, followed by a plateau indicating the near-complete release of the drug within 10 hours.

In stark contrast, the imidacloprid-loaded CS-DS NPs demonstrated a markedly different release profile, indicative of a controlled-release system. The initial release was moderate, with about 50% of the drug being released over the first 10 hours. This was followed by a sustained release phase, where the remaining drug was gradually released, reaching the majority release by the 55-hour mark. This prolonged release profile from the CS-DS nanocarrier was significantly slower compared to the rapid release in deionized water, highlighting the controlled-release capabilities of the nanoformulation.

The distinct release profile of the imidacloprid-loaded CS-DS NPs, characterized by a slower and more sustained drug release rate, substantiates our claim of a controlled-release nanoformulation. The revised Fig. 9 and the accompanying kinetic analysis, which will be provided in the supplementary materials, offer a comprehensive view of the controlled-release behavior of the CS-DS NP system."

3.2. Toxicological studies

Table 1 shows the tolerance of *S. littoralis* caterpillars to imidacloprid-loaded CS-DS NPs and unloaded imidacloprid. There is an obvious link between the toxicology of pesticides and their treatment time, with toxicity arising as exposure duration rises. Imidacloprid-loaded CS-DS NPs were more hazardous than imidacloprid alone. Within 24 and 48 hours of therapy, imidacloprid-loaded CS-DS NPs were about 2.2 times as toxic as unloaded imidacloprid to *S. littoralis* larvae, with LC_{50} values of 146.923 and 334.159 ppm, respectively. After 72 and 120 h of treatments, imidacloprid-loaded CS-DS NPs were about four times as toxic as unloaded imidacloprid, with LC_{50} of 74.896 and 301.229 ppm, respectively. After 120 h of treatment, the LC_{50} values were 67.218 and 273.981 ppm for imidacloprid and imidacloprid-loaded CS-DS NPs, respectively. Statistically, there was a statistically significant difference ($P < 0.05$) between the LC_{50} of treatment with unloaded imidacloprid and that of imidacloprid-loaded CS-DS NPs at each treatment period, as the 95% confidence limits did not overlap.

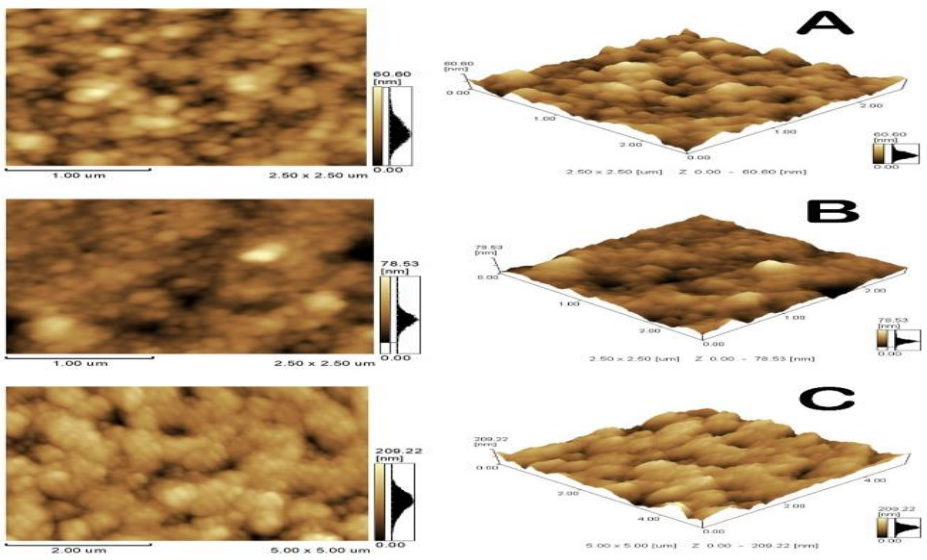

Fig. 5. AFM images for (A) imidacloprid, (B) CS-DS NPs, and (C) imidacloprid-Loaded CS-DS NPs

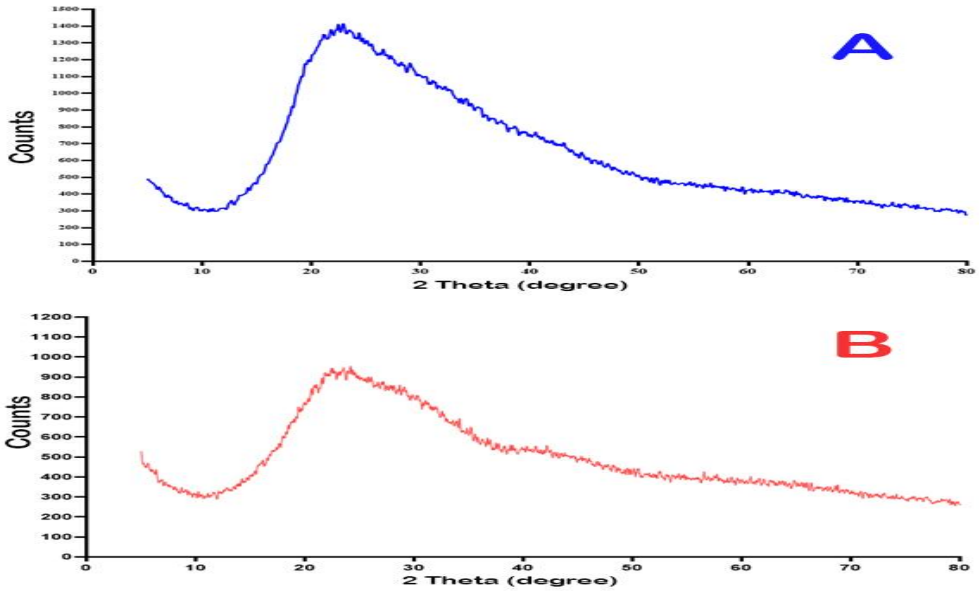

Fig. 6. XRD for (A) CS-DS NPs and (B) imidacloprid-loaded CS-DS NPs

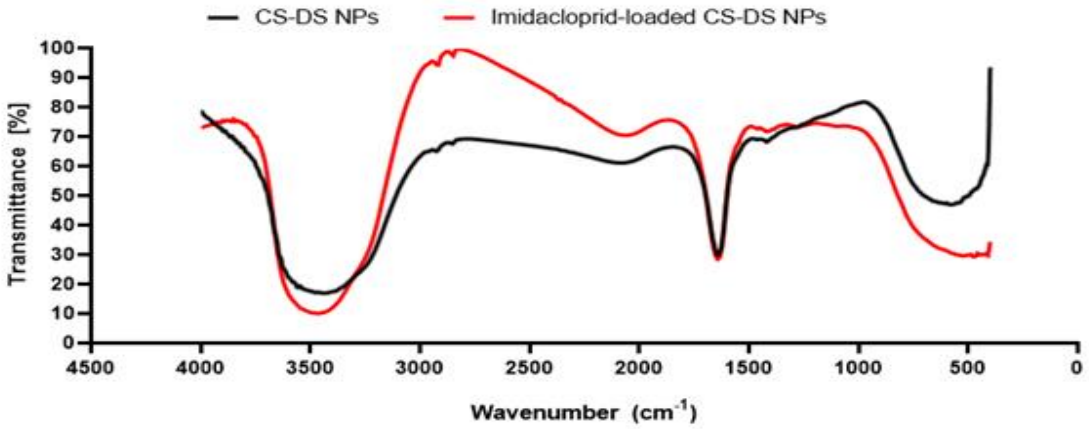

Fig. 7. FTIR for CS-DS NPs and imidacloprid-Loaded CS-DS NPs

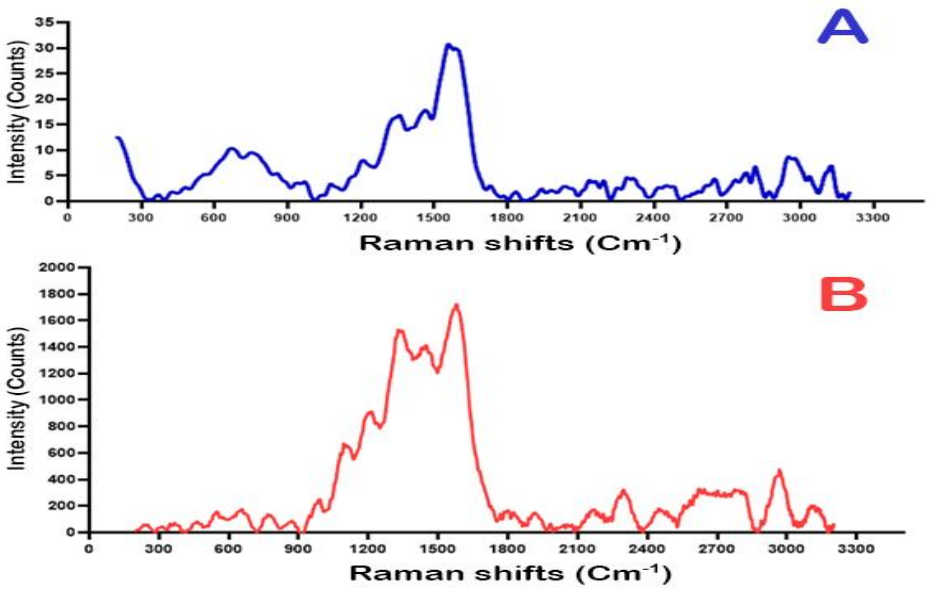

Fig. 8. Raman spectra for (A) CS-DS NPs and (B) imidacloprid-Loaded CS-DS NPs

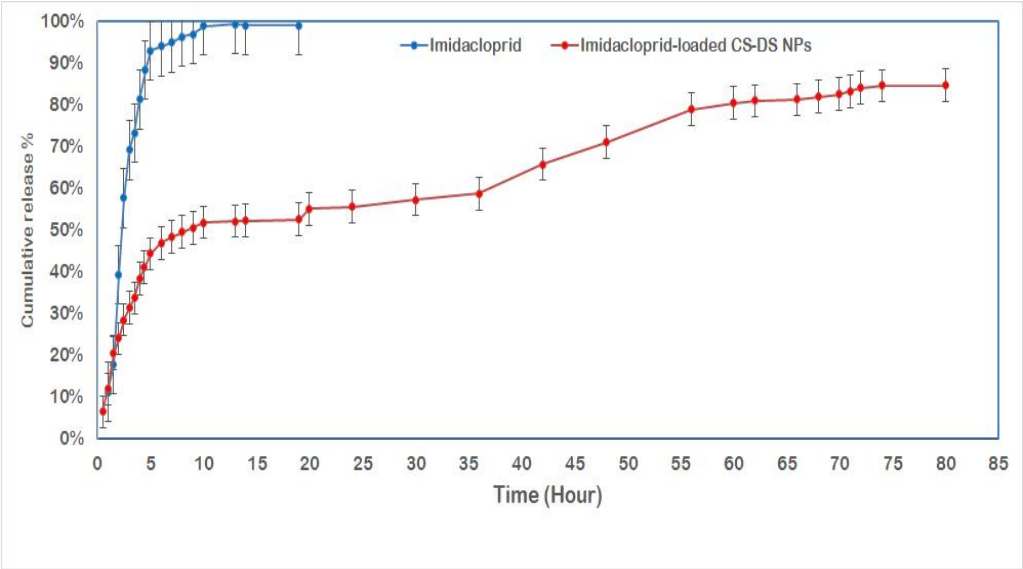

Fig. 9. In vitro release study of imidacloprid from water and from imidacloprid-loaded CS-DS NPs

Table 1. Susceptibility of *S. littoralis* larvae, treated as 4th-instars, to unloaded imidacloprid and imidacloprid-loaded CS-DS NPs

Time of treatment (hr)	Unloaded imidacloprid				Imidacloprid-loaded CS-DS NPs				
	LC_{50} (ppm) (95% CL)	Slope ± SD	$\chi^2_{(df)}$	P	LC_{50} (ppm) (95% CL)	Slope ± SD	$\chi^2_{(df)}$	P	Toxicity index (%)
24	490.66 (418.62 - 599.78)	1.30 ± 0.22	$10.16_{(11)}$	0.900	272.15 (211.90 - 321.57)	1.36 ± 0.22	$14.96_{(11)}$	0.900	55.46
48	334.16 (272.78 - 391.26)	1.31 ± 022	$11.86_{(11)}$	0.900	146.92 (103.18 - 183.26)	1.82 ± 0.24	$30.05_{(11)}$	0.005*	43.96
72	301.23 (228.00 - 362.52)	1.14 ± 0.22	$16.26_{(11)}$	0.900	74.90 (40.26 - 105.28)	2.48 ± 0.39	$32.38_{(11)}$	0.005*	24.86
120	273.98 (208.45 - 327.09)	1.26 ± 0.22	$20.81_{(11)}$	0.050*	67.22 (32.34 - 98.53)	2.41 ± 0.40	$28.01_{(11)}$	0.005*	24.53

95% CL: 95% confidence limits; CS-DS NPs: chitosan-dextran sulfate nanoparticles; * significant heterogeneity at P <0.05; data were estimated using three replicates of a pool of 20 larvae each.

Table 2. Imidacloprid concentrations in different body organs of *S. littoralis* larvae treated as 4th-instars for five days with the LC_{50} of unloaded imidacloprid and imidacloprid-loaded CS-DS NPs.

Organs	Unloaded imidacloprid (ppm)		Imidacloprid-loaded CS-DS NPs (ppm)	
	Imidacloprid	%#	Imidacloprid	%#
Brain	42.644 ± 1.35[a]	15.564 ± 0.857[a]	41.164 ± 0.270[a]	61.238 ± 0.697[a*]
Hemolymph	17.483 ± 0.700[b]	6.381 ± 0.442[b]	21.778 ± 0.352[b*]	32.398 ± 0.909[b*]
gut	69.119 ± 1.67[c]	25.227 ± 1.057[c]	50.711 ± 0.385[c*]	75.439 ± 0.994[c*]
Total Body	115.684 ± 0.02[d]	42.223 ± 0.165[d]	53.062 ± 0.480[d*]	78.937 ± 1.23[d*]

CS-DS NPs: chitosan-dextran sulfate nanoparticles. # % concentration of imidacloprid relative to the applied LC_{50}. Data are presented as the mean ± SD (n=3). Means within columns followed by different letters are significantly different ($p<0.05$), using the Tukey test. * Significant difference ($p<0.05$) between imidacloprid concentration in unloaded imidacloprid and imidacloprid-loaded CS-NPs per each organ separately, using Student's *t*-test

3.3. Biochemical studies

3.3.1. Distribution of unloaded imidacloprid and imidacloprid-loaded CS-DS NPs in different body organs

In different body organs of *S. littoralis* larvae treated as 4th-instars, the concentrations of imidacloprid in imidacloprid-loaded CS-DS NPs were higher than those in unloaded imidacloprid. In imidacloprid-loaded CS-DS NPs treatment, the concentrations in descending order were as follows: whole body > alimentary canal > brain > hemolymph ($p<0.05$). The same pattern was also found for unloaded imidacloprid **(Table 2)**. The concentration of imidacloprid in imidacloprid-loaded CS-DS NPs treatment in the whole body reached 78.93% of the applied sub-lethal dose (LC_{50}), while in unloaded imidacloprid it was 42.22% ($p < 0.001$, df = 4, t = 51.465).

3.3.2. Levels of energy reserves

Protein ($P < 0.001$, df = 2, 6, F = 223.332), carbohydrate ($P < 0.001$, df = 2, 6, F = 1071.481), and lipid ($P < 0.001$, df = 2, 6, F = 4158.134) contents were significantly decreased in the *S. littoralis* larvae treated with the LC_{50} of imidacloprid-loaded CS-DS NPs as compared to the control group by 0.42, 2.15 and 2.27-fold, respectively **(Fig. 10)**. Also, there was a significant decrease in larvae treated with imidacloprid-loaded CS-Ds NPs compared to the unloaded imidacloprid for protein, carbohydrate, and lipid contents by 0.3, 1.93 and 1.26-fold, respectively.

3.3.3. Levels of oxidative stress markers

Fig. 11 shows that treatment of *S. littoralis* larvae by LC_{50} of imidacloprid-loaded CS-DS NPs induced a significant increase in the lipid peroxidation process (increased MDA concentration) in the larval tissues, compared to the control by 3.5-fold, ($P = 0.04$, df = 2, 6, F = 14.576). In contrast, lipid peroxidation levels in unloaded imidacloprid did not change compared to the control ($P = 0.214$, df = 2, 6, F = 14.576). The concentration of MDA due to treatment with imidacloprid-loaded CS-DS NPs was significantly higher than that due to treatment with unloaded imidacloprid (2-fold, p= 0.033, df-6,8, F=14.576).

In contrast, there was a significant decline in the level of GSH in larvae treated with imidacloprid-loaded CS-DS NPs by 42.30% ($P = 0.001$, df = 2, 6), F = 26.839) and unloaded imidacloprid by 30.76%, ($P = 0.004$, df = 2, 6, F = 26.839), compared to the control group.

There was a change in GSH level between imidacloprid-loaded CS-DS NPs and unloaded imidacloprid treatments ($P = 0.260$, df = 2, 6, F = 26.839) **(Fig. 11).**

3.3.4. Antioxidant enzyme activities

Fig. 12 Shows that the activities of antioxidant enzymes (CAT, SOD, and APOX) in *S. littoralis* larvae treated with imidacloprid-loaded CS-DS NPs and unloaded imidacloprid were significantly higher than those in control groups. CAT activity in imidacloprid-loaded CS-DS NPs treatment increased by 67.40% of the control ($p < 0.001$, df = 2, 6, F = 300.629). The CAT activity in imidacloprid-loaded CS-DS NPs treatment was also significantly higher than that in unloaded imidacloprid treatment by 30.08% ($p < 0.001$, df = 2, 6, F = 300.629). The activity of SOD in imidacloprid-loaded CS-DS NPs and unloaded imidacloprid treatment was significantly higher than that in the control group by 1.23-fold and 1.055-fold, respectively ($P < 0.001$, df = 6 ,8, F = 53.351).

There was no change in SOD activity between treatments with unloaded imidacloprid and imidacloprid-loaded CS-DS NPs ($P = 0.57$, df = 2, 6, F = 53.351).

APOX activity significantly increased by 19.67% ($P = 0.003$, df = 2, 6, F = 17.863) and 15.63% ($P = 0.010$, df = 2, 6, F = 17.863) in treatments with imidacloprid-loaded CS-DS NPs and unloaded imidacloprid, respectively, compared to control larvae. There was no change in APOX activity between treatments with imidacloprid-loaded CS-DS NPs and unloaded imidacloprid ($P = 0.519$, df = 2, 6, F = 17.863).

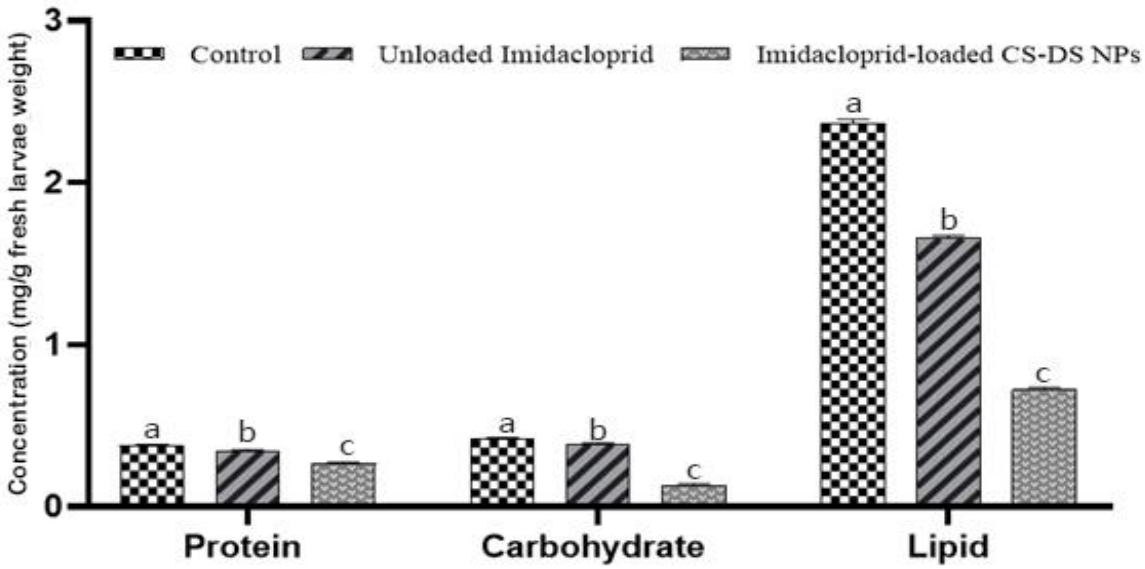

Fig. 10. Total protein, carbohydrate and lipid contents of *S. littoralis* larvae treated as 4th-instars for five days with the LC_{50} of imidacloprid-loaded CS-DS NPs and unloaded imidacloprid. Data are presented as the mean ± SD (n = 3). Means followed by different letters per each nutrient separately are significantly different ($p<0.05$), using Tukey's test. CS-DS NPs: chitosan dextran sulfate nanoparticles

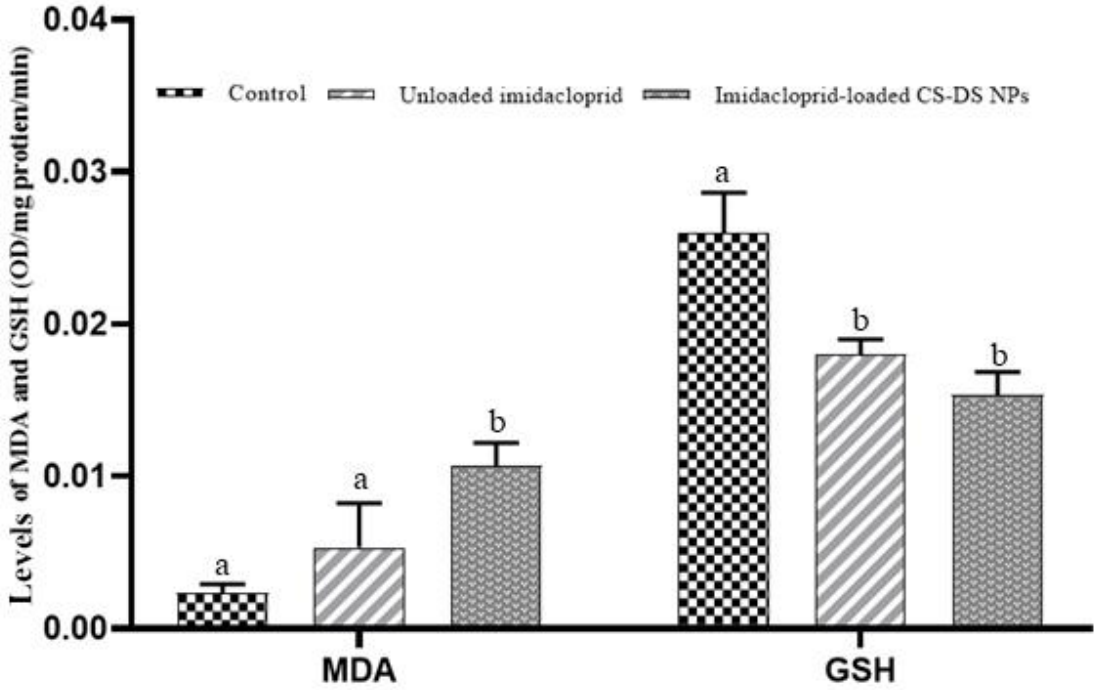

Fig. 11. Malondialdehyde (MDA) and reduced glutathione (GSH) levels of *S. littoralis* larvae treated as 4th-instars for five days with the LC_{50} of imidacloprid-loaded CS-DS NPs and unloaded imidacloprid. Data are presented as the mean ± SD (n = 3). Means followed by different letters per each antioxidant marker separately are significantly different ($p<0.05$), using Tukey's test. CS-DS NPs: chitosan dextran sulfate nanoparticles

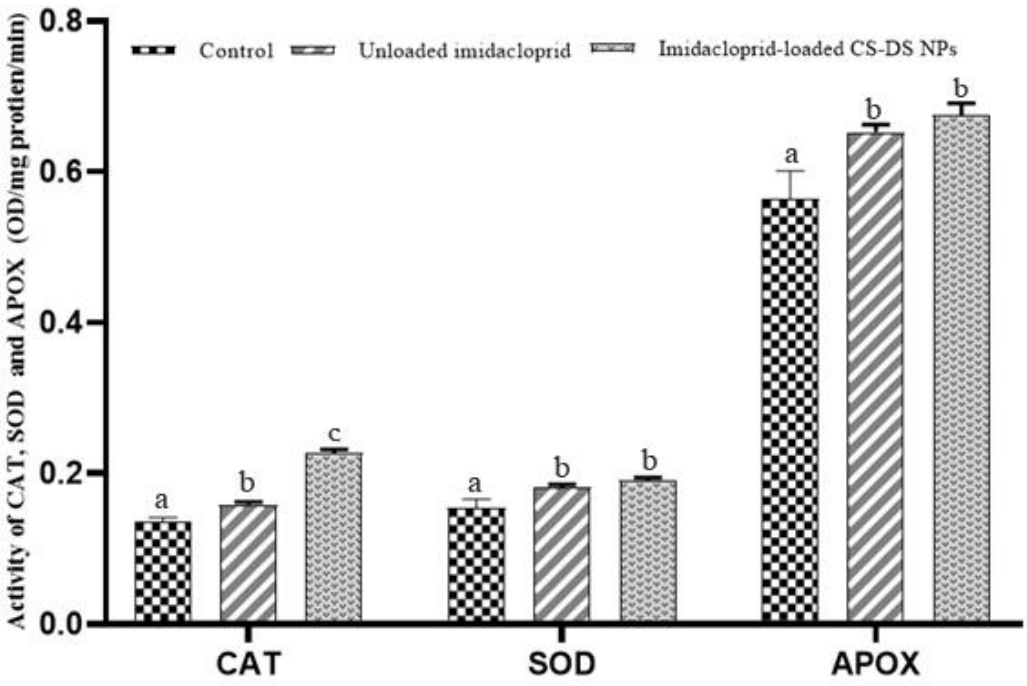

Fig. 12. Ascorbate peroxidase (APOX), superoxide dismutase (SOD), and catalase (CAT) activities of *S. littoralis* larvae treated as 4th-instars for five days **with** the LC_{50} of **imidacloprid-loaded CS-DS NPs and unloaded imidacloprid. Data are presented as the mean ± SD (n = 3). Means followed by different letters per each antioxidant enzyme separately are significantly different (p<0.05), using Tukey's test. CS-DS NPs: chitosan dextran sulfate nanoparticles**

3.3.5. Detoxification enzyme activities

The activity of AChE in *S. littoralis* larvae treated with imidacloprid-loaded CS-DS NPs was decreased by 63.9% (P < 0.001, df = 2, 6, F = 48.649) versus 42.2% in larvae treated with unloaded imidacloprid (P = 0.004, df = 2, 6, F = 48.649) compared to the activity in control larvae. Significant decrease of AChE activity in imidacloprid-loaded CS-DS NPs by 37.56% compared to that in unloaded imidacloprid has been recorded (P = 0.009, df = 2, 6, F = 48.649) **(Fig. 13).**

The application of imidacloprid-loaded CS-DS NPs to *S. littoralis* larvae resulted in a significant increase in GST activity as compared to the unloaded imidacloprid and control groups by 1.47-fold and 1.72-fold, respectively (P < 0.001, df = 2, 6, F = 112.028), respectively. However, there was no change in the GST activity of larvae treated with unloaded imidacloprid compared to that in the control group (P = 0.145, df = 2, 6, F = 112.028) **(Fig. 13).**

3.3.6. Nitric oxide level

The level of NO significantly increased in *S. littoralis* larvae exposed to LC_{50} of imidacloprid-loaded CS-DS NPs and unloaded imidacloprid, compared to control larvae. This increase was 2.34-fold and 1.65-fold, respectively (P < 0.001, df = 2, 6, F = 150.890). Also, there was a significant increase by 1.41-fold in NO activity for larvae treated with imidacloprid-loaded CS-DS NPs compared to that in larvae treated with unloaded imidacloprid (P < 0.001, df = 2, 6), F = 150.890) **(Fig. 14).**

4. Discussion

This is, to the best of our knowledge, the first report demonstrating quantitatively that imidacloprid in a nanoparticle formulation loaded on a chitosan nanocarrier disrupts survival and multiple metabolic processes of *S. littoralis*, leading to its control via a novel approach.

Transmission electron microscopy (TEM) is utilized to determine the size and distribution of nanoparticles in a quantifiable manner [46]. TEM image demonstrated the successful formation of homogeneous CS-DS NPs (average nano-size = 74.90 ± 7.3 nm) and imidacloprid-loaded CS-DS NPs (average nano-size = 97.42 ± 7.86 nm). The main shapes of the two nanoformulations were virtually spherical, with small aggregations. The thick layer of CS-DS NPs visible in the TEM image revealed that imidacloprid-loaded CS-DS NPs had successfully formed.

Dynamic light scattering (DLS) determines the hydrodynamic size of particles using the light scattering mechanism of a laser passing through a colloidal solution and analyzing the modification of the intensity of scattered light as a function of time [47]. Imaging and particle size analysis increased from 142 nm to about 165 nm, correlating with the

DLS results that the imidacloprid-loaded CS-DS NPs were larger than the CS-DS NPs. The result was in line with Chavan et al. [48] for loaded ciprofloxacin drug on the same nanocarrier CS-DS NPs and Fathy et al. [28] for silica-coated insulin-loaded chitosan nanoparticles. By comparing DLS and TEM image data, the diameter of particles determined by DLS is significantly larger compared to the size analysis performed by TEM because the suspension is in aggregated form, as explained by Raval et al. [49] for determination of nanoparticles aggregation state.

The ability of nanoparticles to change surface shape is important in vivo [48]. Spherical shapes could improve the delivery of drugs. In line with Kaur et al. [50], CS-DS NPs and imidacloprid-loaded NPs have well-defined, spherical nanoparticles in a typical SEM data set. Also, in agreement with Alfy et al. [51], they found chitosan nanoparticles to be typically spherical and some agglomerated. The imidacloprid-loaded CS-DS NPs were larger than CS-DS NPs, probably due to drug loading during preparation.

A nanoparticle's surface charge is represented by its zeta potential. It indicates the electric potential of nanoparticles, which is affected by particle structure as well as the dispersion medium [49]. The zeta potential approach is also regarded as an essential analysis to evaluate the nanoparticle's colloidal stability [52]. Consequently, CS-DS NPs and imidacloprid-loaded CS-DS NPs showed more colloidal stability, as indicated by their measured zeta potential values of 30.28 ± 3.35 and 20.70 ± 3.59 mV, respectively.

There is a relation between NP surface roughness and cellular attachment [52]. The circular muscle layer and the epithelial layer of the midgut of *S. littoralis* were damaged by imidacloprid exposure [7,54]. They suggested that the insecticide particles can be trapped on rough surfaces, altering epithelial cell permeability. Thus, the gut cells interact with the very rough surfaces of any formulation, decreasing their in vivo stability. As determined by AFM, the low roughness (1.42±0.53 nm) of imidacloprid-loaded CS-DS NPs confirms their high bioavailability.

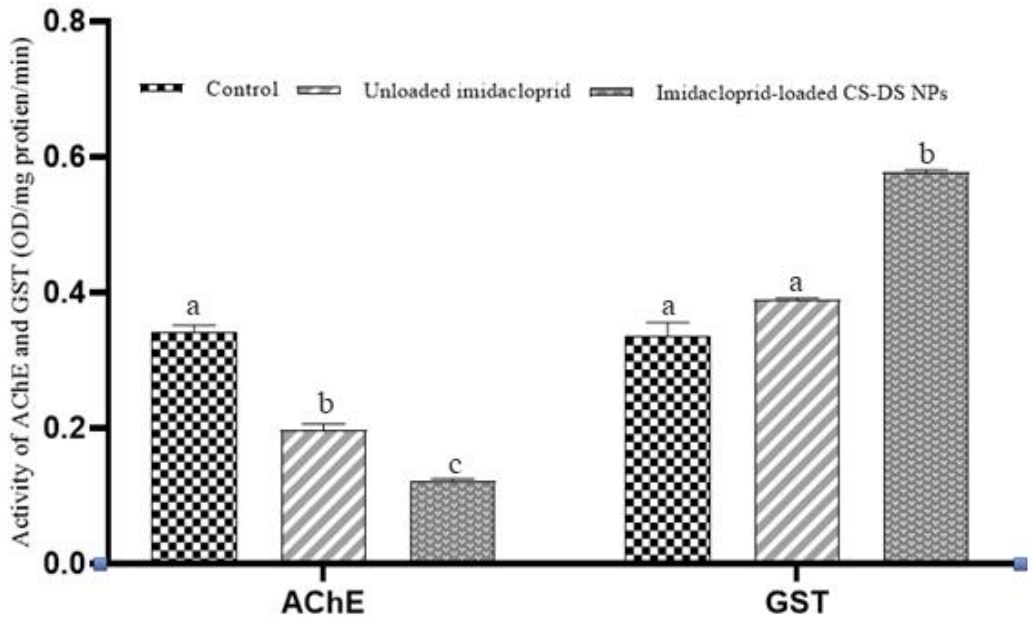

Fig. 13. Acetylcholinesterase (AChE) and glutathione S-transferase (GST) levels of *S. littoralis* larvae treated as 4th-instars for five days **with** the LC_{50} of **imidacloprid-loaded CS-DS NPs and unloaded imidacloprid. Data are presented as the mean ± SD (n = 3). Means followed by different letters per each detoxification enzyme separately are significantly different (p<0.05), using Tukey's test. CS-DS NPs: chitosan dextran sulfate nanoparticles**

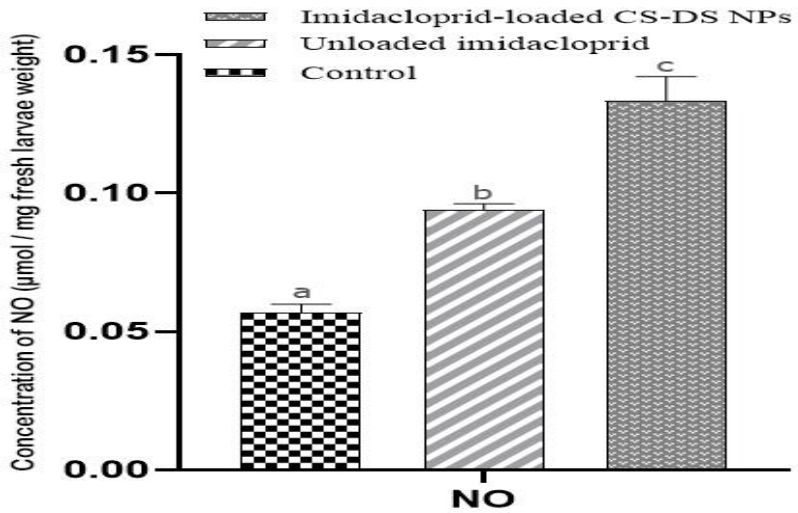

Fig. 14. Nitric oxide (NO) level of *S. littoralis* larvae treated as 4th-instars for five days with the LC_{50} of imidacloprid-loaded CS-DS NPs and unloaded imidacloprid. Data are presented as the mean ± SD (n = 3). Means followed by different letters are significantly different ($p<0.05$), using Tukey's test. CS-DS NPs: chitosan dextran sulfate nanoparticles

Energy-dispersive X-ray Spectrometer (EDX) resulting in imidacloprid-loaded CS-DS NPs were identical to those of CS-DS NPs with the chloride element as a dominant element, in line with Singh et al. [25].

The powder XRD patterns exhibited a prominent diffraction peak at an angle of 2θ = 22.44º for CS-DS NPs and 23.54º for imidacloprid-loaded CS-DS NPs. These diffraction peaks appear to be very broad because of the amorphous nature of imidacloprid and chitosan nanoparticles; the same results were obtained by Li [55] for chitosan dextran and their nanocomposites.

Analysis of FTIR spectra of unloaded imidacloprid result has the same peaks observed by Adak et al. [13], Gao et al. [56] and Moradi et al. [57]. Similar findings have been reported by Nirmala et al. [58] and Fathy et al. [28]. The broadening of peaks at 3400 cm^{-1} indicates hydrogen bond formation between CS-DS NPs and imidacloprid during interaction, supporting previous studies by Memarizadeh et al. [59], Chavan et al. [48] and Hong et al. [60].

The Raman spectrum of imidacloprid-loaded CS-DS NPs was similar to that of CS-DS NPs. Also, the peak at 1447 cm^{-1} indicates hydrogen bonding between CS-DS NPs and the imidacloprid molecule. The same results were obtained by Moreira et al. [15] and Al-Syadi et al. [61] for imidacloprid and by Li [62] for chitosan dextran NPs.

Higher effectiveness of encapsulation (67.824%). Therefore, when the positively energized imidacloprid molecule is initially mixed with the inversely charged DS before being introduced to CS, it is anticipated that an electrical attraction will develop between both of the inversely charged molecules. In addition to any possible electrostatic interaction between the highly charged CS and DS molecules, this will lead to improved encapsulation efficiency [63]. Imidacloprid-loaded CS-DS NPs within pH ten were evaluated for GIT media release of *S. littoralis* midgut. Imidacloprid-loaded CS-DS NPs released slowly and sustainably in deionized water compared to unloaded formulations in line with Adak et al. [13], Qian et al. [64], and Memarizadeh et al. [59]. Imidacloprid's limited release is due to CS-DS NP loading. The lowering surface roughness values of imidacloprid-loaded CS-DS NPs show that CS-DS NP carriers decrease surface porosity [28]. That reduces imidacloprid release, suggesting that the nanocarrier CS-DS encapsulates the drug along its trip through pH-varying GIT [65].

Traditional and sustained-release insecticides based on nanocarriers were used to compare their LC_{50} values against *S. littoralis*. Treatment with imidacloprid-loaded CS-DS NPs (LC_{50} = 67.22 ppm) can save up to 75% of imidacloprid used versus unloaded imidacloprid (LC_{50} = 273.98 ppm) in *S. littoralis* larvae management. Sabbour [66] found that the LC_{50} of imidacloprid-loaded CS-DS NPs was about four times as toxic as unloaded imidacloprid in *Ceratitis capitata* and *Pryas oleae*. These results agree with the findings of Sabbour and Shaurub [67] in that nano-imidacloprid was about 1.2 times as toxic as imidacloprid to *Bactrocera oleae* 3rd larval instars under laboratory conditions.

The present results demonstrated that feeding 4th-instar larvae of *S. littoralis* to sublethal concentrations of imidacloprid-loaded CS-DS NPs and unloaded imidacloprid resulted in a significant decrease in protein, carbohydrate, and lipid content compared to the control groups. Similar results were obtained by El-Saleh et al. [68], who treated *S. littoralis* with the neonicotinoids insecticides

thiamethoxam, thiacloprid, imidacloprid, and acetamiprid.

Protein is reduced by insecticidal stress because it is broken down into free amino acids. Thus, these amino acids will assist in providing energy for the insect when they enter the Krebs cycle as keto acids [69]. According to Canavoso et al. [70], the amount of lipid accessible for the energy reserve appears to be the outcome of a balance between the intake of food and the demand for reserve made by functions like growth, maintenance, and reproduction. Any hazardous substance upsets this equilibrium. According to Remia et al. [71], the decrease in carbohydrates raises the prospect of active glycogenolysis and glycolytic pathways producing additional energy during stressful situations.

Pesticides raise the amounts of superoxide ($O_2^{\bullet-}$) and NADPH oxidases (NOXs), thereby increasing ROS signaling within the cell. Insecticide-treated insects frequently produce ROS, which may be the cause of their death. However, defensive enzymes allow the insects to overcome the ROS produced [72]. High ROS can cause the oxidation of proteins, lipids, and DNA, which can have various harmful effects. Several studies found that pesticide resistance is mostly caused by enhanced detoxifying enzyme activity [72,73]. The results confirm that herbivorous insect pests defend against exogenous and endogenous oxidative radicals by increasing antioxidant concentrations.

Antioxidant enzymes maintain a balanced metabolism and regulate oxidative stress in insects. Many detoxifying enzymes, including glutathione peroxidase (GPX), GST, CAT, SOD, GSH, and others, have been found in *S. littoralis* and have been shown to occur in insects as a defense against oxidative stress [72]. Enzymatic assays in the current study demonstrated that larvae fed on sublethal concentrations of imidacloprid-loaded CS-DS NPs and unloaded imidacloprid had higher levels of immune response (NO), detoxification enzymes (GST), antioxidative defense (SOD, APOX, and CAT), and important oxidative status markers (MDA and GSH) than controls. Similar results were obtained by El Saleh et al. [68] for *S. littoralis* treated with thiamethoxam, thiacloprid, imidacloprid, and acetamiprid .

The current study determined lipid peroxidation (LPO) levels by measuring the concentration of MDA. MDA is the resultant compound derived from LPO, performing as an indication of cellular membrane breakdown resulting from the occurrence of oxidative stress [10,74]. The MDA level of *S. littoralis* larvae exposed to sublethal concentrations of imidacloprid-loaded CS-DS NPs exhibited a significant increase compared to the control. Several studies revealed increased levels of MDA and ROS in *Apis mellifera* after treatment with imidacloprid [10,74]. Furthermore, in imidacloprid-treated *S. littoralis* larvae, elevated levels of MDA were concomitant with elevated levels of CAT, SOD, and GST. This might have been an attempt to counterbalance the increase in MDA levels as a protective strategy by cells against the formation of free radicals [75].The current results align with those of Balieira et al. [74], who reported elevated levels of MDA and SOD and CAT following the exposure of honeybees to imidacloprid.

Current results show no difference in the GSH of larvae treated with unloaded imidacloprid and CS-DS NPs loaded with imidacloprid. GSH plays a vital role in preserving the cell's redox state. It interacts with H_2O_2 and hydroxyl radicals to reduce their cellular toxicity. GSH prevents peroxidative damage to cell membranes and keeps many proteins' sulfhydryl groups in their reduced forms by decreasing peroxides [76]. Additionally, GSH functions as a cofactor for antioxidant enzymes such as glutathione transferase peroxidase and dehydroascorbate reductase, as well as a non-enzymatic radical scavenger [77]. The two molecules of GSH participate in producing one molecule of the oxidized form (glutathione disulfide) during oxidative stress, which lowers the total amount of glutathione overall [78]. In agreement with the current results, earlier studies documented increased GHS levels after exposure to toxic xenobiotics [79,80].

Compared to the controls, the levels of CAT, SOD, and APOX increased in larvae treated with imidacloprid-loaded CS-DS NPs and unloaded imidacloprid. Enzymes with antioxidant properties like CAT, SOD, and peroxidases frequently become more active when ROS levels are elevated [81]. These are the main enzymes in the antioxidant system that scavenge radicals from oxygen [82,83]. They've been related to toxicity from pesticides [84,85]. According to Sofo et al. [86], SODs are believed to offer a first line of defense against oxygen radicals, particularly the main ROS produced by mitochondrial respiration and different metabolic processes, superoxide anion ($O_2^{\bullet-}$). At the same time, CAT, which is present in peroxisomes, catalyzes the conversion of two molecules of H_2O_2 into O_2 and two molecules of H_2O; the SODs eliminate the potentially harmful superoxide anions from biological systems by converting them to H_2O_2. Poiani et al. [21] concluded that imidacloprid affects the redox balance and the defense system of *S. littoralis* larvae.

GST is a primary and secondary metabolic enzyme related to insect resistance against insecticides, as it plays an essential role in detoxifying heterologous compounds [87]. The increased activity of GST in the present study after treatment with imidacloprid suggests that this

enzyme might be involved in the detoxifying mechanism by the addition of GSH to various electrophilic toxic secondary metabolites to form more hydrophilic nontoxic or low-toxic substances [88]. A significant increase in GST level obtained with imidacloprid-loaded CS-DS NPs compared to both unloaded imidacloprid and control group is in line with Hamama et al. [30], who recorded increased GST activity in 4th-instar larvae of *S. littoralis* treated with imidacloprid. However, El-Saleh et al. [68] found that the activity of GST did not change in *S. littoralis* larvae treated with imidacloprid.

S. littoralis larvae treated with imidacloprid-loaded CS-DS NPs had the lowest levels of AChE activity. Similarly, decreased AChE activity has been reported in *S. littoralis* [68] and *Apies mellifera* [62,89] treated with imidacloprid. In contrast, the application of imidacloprid to the 4th-instar larvae of *S. littoralis* resulted in a significant increase in AChE activity compared to the control group [30]. Imidacloprid is classified as a highly neuroactive insecticide due to its ability to induce toxicity in insect pests by disrupting neuronal transmission at post-synaptic nicotinic acetylcholine receptors (nAChRs) [4, 90]. The existence of various subtypes of nAChRs has been identified as the underlying causes of the harmful effects induced by different insecticides. Imidacloprid selectively interacts with nAChRs, exhibiting binding affinity towards four subtypes of nAChRs of the insect brain– Dα1, Dα2, Dβ1, and Dβ2 [91].

Nitric oxide (NO) is a reactive nitrogen species (RNS) derivative [92], Belonging to a category of nitrogen moieties that have strong bonds with oxygen [93]. Although NO plays vital roles in certain physiological regulations (e.g., neural and cardiovascular activities), it harms the cells if produced and presents excessively because of its strong reaction to extra free radicals, such as $O_2^{\cdot-}$ [94]. Once NO or similar species are produced after exposure to certain xenobiotic agents, such as pesticides, nitrosative stress may result. [95]. The current investigation demonstrated increased NO activity in *S. littoralis* larvae treated with imidacloprid-loaded CS-DS NPs and unloaded imidacloprid. The activated NO concentrations imply its role as an immune response molecule against recently synthesized pesticides [96]. Inducible NO synthase catalyzes NO production from arginine [97]. Inducible NO (iNO) acts as a cytotoxic free radical and nitrergic signaling molecule that defends against stressful circumstances [97,98]. Furthermore, iNO reacts with H_2O_2 to form hydroxyl radical (OH) and with O_2^- to form peroxynitrite (ONOO−). These radicals markedly contribute to the overall anti-cytotoxic functions [98].

5. Conclusion

The findings of this research indicate that the nanoformulation of chitosan-dextran sulfate (CS-DS NPs) encapsulating imidacloprid represent a highly effective and promising approach for the management of the *S. littoralis* pest. The imidacloprid-loaded CS-DS NPs exhibited superior properties, such as optimal nano-size as evidenced by TEM imaging and DLS data, along with colloidal stability as suggested by zeta potential measurements and AFM analysis. Notably, the encapsulation efficiency peaked at a pH conducive to the loading method, with the imidacloprid-loaded CS-DS NPs demonstrating a sustained release of imidacloprid at a pH of 10, which aligns with the internal environment of *S. littoralis*. Furthermore, the study establishes that the imidacloprid-loaded CS-DS NPs outperform the non-encapsulated imidacloprid formulations in terms of inducing greater toxicity and more significant biochemical changes (elevation of oxidative stress markers, and decrease of antioxidant enzyme, and AChE activities) in the target pest. From an applied perspective, the heightened toxicity (reflected in a lower LC50 value) suggests potential benefits such as reduced application costs, diminished environmental impact, lesser harm to beneficial pollinators, and a slower rate of resistance development.

6. Statements & Declarations

Conflict of interest: The authors declare no competing interests.

Informed consent: Consent to participate and consent to publish were obtained from all individual participants included in the study.

Authors' contribution: All authors participated in collecting the literature, managing the manuscript, and accepting the final version of the article.

Funding: This work was funded by Faculty of Science, Cairo University, Egypt.

Availability of data and materials: All data needed to support the conclusions are included in this article. Additional data related to this paper can be requested from the corresponding author (heshamyousef.eg@cu.edu.eg).

Graphics program used: GraphPad Prism 8

Acknowledgments

I'm grateful to all of those with whom I have completed this work. Dr. Mostafa Mahmoud, Entomology Dept. Faculty of Science, Cairo University, for his help and advice in statistics analysis. Dr. Mohamed El-Nems, General Manager of El-Nems Services Company, for his help in providing Imidacloprid insecticide. Dr. Nashwa Saied and Dr. Shimaa Nagiub for providing insect culture.

7. References

[1] Kandil, M.A., Abdel-Aziz, N.F., and Sammour, E.A., (2003). Comparative toxicity of chlorofluazron and leufenuron against cotton leaf worm, Spodoptera littoralis (Boisd). *Egyp. J. Agric. Res. NRC 2*: 645-661.

[2] CABI, (2022). *Spodoptera littoralis* (cotton leafworm). From https://www.cabidigitallibrary.org/doi/10.1079/cabicompendium.51070#core-ref 69. Accessed 22 August 2022

[3] Kohl, K.L., Harrell, L.K., Mudge, J.F., Subbiah, S., Kasumba, J., Osma, E., Barman, A.K., and Anderson, T.A., (2019). Tracking neonicotinoids following their use as cotton seed treatments. *PeerJ*, 7:e6805. https://doi.org/10.7717/peerj.6805

[4] Nugnes, R., Russo, C., Orlo, E., Lavorgna, M., and Isidori, M., (2023). Imidacloprid: Comparative toxicity, DNA damage, ROS production and risk assessment for aquatic non-target organisms. *Environmental Pollution*, *316*. https://doi.org/10.1016/j.envpol.2022.120682

[5] Si, F., Zou, R., Jiao, S., Qiao, X., Guo, Y., and Zhu, G., (2018). Inner filter effect-based homogeneous immunoassay for rapid detection of imidacloprid residue in environmental and food samples. *Ecotoxicology and Environmental Safety* 148: 862-868. https://doi.org/10.1016/j.ecoenv.2017.11.062

[6] Sabry, A.H., Salem, H.A-N., and Metwally, H.M., (2021). Development of imidacloprid and indoxacarb formulations to nanoformulations and their efficacy against Spodoptera littoralis (Boisd). *Bulletin of the National Research Centre*, *45*(1). https://doi.org/10.1186/s42269-020-00477-8

[7] Shaurub, El. H., Tawfik, A.I., and El-Sayed, A.M., (2023). Individual and combined treatments with imidacloprid and spinosad disrupt survival, life-history traits, and nutritional physiology of *Spodoptera littoralis*. Inter. J. Tropical Insect Sci. 43: 737-748. https://doi.org/10.1007/s42690-023-00982-z

[8] Horowitz, A.R., and Ishaaya, I., (2004). Biorational Insecticides — Mechanisms, Selectivity and Importance in Pest Management. In: Horowitz AR, and Ishaaya I (eds) Insect Pest Management. Springer, Berlin, Heidelberg. https://doi.org/10.1007/978-3-662-07913-3_1

[9] Zheng, Q., Niu, Y., and Li, H., (2016). Synthesis and characterization of imidacloprid microspheres for controlled drug release study. *Reactive and Functional Polymers 106*: 99-104 https://doi.org/10.1016/j.reactfunctpolym.2016.07.006

[10] He, B., Liu, Z., Wang, Y., Cheng, L., Qing, Q., Duan, J., Xu, J., Dang, X., Zhou, Z., and Li, Z., (2021). Imidacloprid activates ROS and causes mortality in honey bees (*Apis mellifera*) by inducing iron overload. Ecotoxicol Environ Saf 228:112709

[11] Singh, A., Dhiman, N., Kar, A.K., Singh, D., Purohit, M.P., Ghosh, D., and Patnaik, S., (2020). Advances in controlled release pesticide formulations: Prospects to safer integrated pest management and sustainable agriculture. In *Journal of Hazardous Materials* (Vol. 385). https://doi.org/10.1016/j.jhazmat.2019.121525

[12] Pathak, V.M., Verma, V.K., Rawat, B.S., Kaurv, B., Babu, N., Sharma, A., Dewali, S., Yadav, M., Kumari, R., Singh, S., Mohapatra, A., Pandey, V., Rana, N., and Cunill, J.M., (2022). Current status of pesticide effects on environment, human health and it's eco-friendly management as bioremediation: A comprehensive review. In *Frontiers in Microbiology* 13. https://doi.org/10.3389/fmicb.2022.962619

[13] Adak, T., Kumar, J., Shakil, N.A., and Walia, S., (2012) Development of controlled release formulations of imidacloprid employing novel nano-ranged amphiphilic polymers. *Journal of Environmental Science and Health - Part B Pesticides, Food Contaminants, and Agricultural Wastes* 47: 217–225. https://doi.org/10.1080/03601234.2012.634365

[14] Yousef, H.A., Fahmy, H.M., Arafa, F.N., Abd Allah, M.Y., Tawfik, Y.M., el Halwany, K.K., El-Ashmanty, B.A., Al-anany, F.S., Mohamed, M.A., and Bassily, M.E., (2023). Nanotechnology in pest management: advantages, applications, and challenges. In *International Journal of Tropical Insect Science* 43: 1387-1399 https://doi.org/10.1007/s42690-023-01053-z

[15] Moreira, A.A.G., De Lima-Neto, P., Caetano, E.W.S., Barroso-Neto, I.L., and Freire, V.N., (2017). The vibrational properties of the bee-killer imidacloprid insecticide: A molecular description. *Spectrochimica acta. Part A, Molecular and biomolecular spectroscopy* 185: 245–255. https://doi.org/10.1016/j.saa.2017.05.051

[16] Malerba, M., and Cerana, R., (2016). Chitosan effects on plant systems. In *International Journal of Molecular Sciences* 17(7). https://doi.org/10.3390/ijms17070996

[17] Chen, Y., Mohanraj, V.J., and Parkin, J.E., (2003). Chitosan-dextran sulfate nanoparticles for delivery of an anti-angiogenesis peptide. *Letters in Peptide Science* 10: 5–6. https://doi.org/10.1007/BF02442596

[18] Ayyaril, S.S., Shanableh, A., Bhattacharjee, S., Rawas-Qalaji, M., Cagliani, R., Shabib, A.G., and Imran khan, M., (2023) Recent progress in micro and nano-encapsulation techniques for

environmental applications: A review. In *Results in Engineering* (Vol. 18). https://doi.org/10.1016/j.rineng.2023.101094

[19] EPA,. (2023). Pesticide Tolerance; Exemptions, Petitions, Revocations, etc.: Addition of Chitosan (Including Chitosan Salts) to the List of Active Ingredients Permitted in Exempted Minimum Risk Pesticide Products. 87 FR 67364 (67364-67371)

[20] Ilhan, A., Gurel, A., Armutcu, F., Kamisli, S., and Iraz, M. (2005). Antiepileptogenic and antioxidant effects of Nigella sativa oil against pentylenetetrazol-induced kindling in mice. *Neuropharmacology* 49: 456-464. https://doi.org/10.1016/j.neuropharm.2005.04.004

[21] Poiani, S.B., Dobeš, P., Kunc, M., Pereira, M.C., Bueno, O.C., and Hyršl, P., (2023). The Influence of Selected Insecticides on the Oxidative Response of Atta sexdens (Myrmicinae, Attini) Workers. *Neotropical Entomology* 52: 1088-1099. https://doi.org/10.1007/s13744-023-01077-7

[22] Büyükgüzel, E., Hyrsl, P., and Büyükgüzel, K., (2010) Eicosanoids mediate hemolymph oxidative and antioxidative response in larvae of Galleria mellonella L. *Comparative biochemistry and physiology. Part A, Molecular & integrative physiology* 156: 176–183. https://doi.org/10.1016/j.cbpa.2010.01.020

[23] López, M.D., Contreras, J., and Pascual-Villalobos, M.J., (2010). Selection for tolerance to volatile monoterpenoids in Sitophilus oryzae (L.), Rhyzopertha dominica (F.) and Cryptolestes pusillus (Schönherr). *Journal of Stored Products Research* 46: 52-58. https://doi.org/10.1016/j.jspr.2009.09.003

[24] Matthews, G., Bateman, R., and Miller, P., (2014). Pesticide Application Methods: Fourth Edition. In *Pesticide Application Methods: Fourth Edition*, Wiley-Blackwell U.S (Vol. 9781118351307). https://doi.org/10.1002/9781118351284

[25] Singh, A., Kar, A.K., Singh, D., Verma, R., Shraogi, N., Zehra, A., Gautam, K., Anbumani, S., Ghosh, D., and Patnaik, S., (2022). PH-responsive eco-friendly chitosan modified cenosphere/alginate composite hydrogel beads as carrier for controlled release of Imidacloprid towards sustainable pest control. *Chemical Engineering Journal* 427. https://doi.org/10.1016/j.cej.2021.131215

[26] Chen, Y., Mohanraj, V.J., Wang, F., and Benson, H.A.E., (2007). Designing chitosan-dextran sulfate nanoparticles using charge ratios. *AAPS PharmSciTech* *8*(4). https://doi.org/10.1208/pt0804098

[27] Cui, F., Zhang, L., Zheng, J., and Kawashima, Y., (2004). A study of insulin-chitosan complex nanoparticles used for oral administration. *Journal of Drug Delivery Science and Technology* 14: 435-439. https://doi.org/10.1016/s1773-2247(04)50081-3

[28] Fathy, M.M., Hassan, A.A., Elsayed, A.A., and Fahmy, H.M., (2023). Controlled release of silica-coated insulin-loaded chitosan nanoparticles as a promising oral administration system. *BMC Pharmacology and Toxicology* 24(1). https://doi.org/10.1186/s40360-02300662-1

[29] Pechenkin, M.A., Balabushevich, N.G., Zorov, I.N., Staroseltseva, L.K., Mikhalchik, E.V., (2011). Design. Vitro and In Vivo Characterization of Chitosan-Dextran Sulfate Microparticles for Oral Delivery of Insulin. J Bioequiv Availab. 3:2 44–50.

[30] Hamama, H.M., Hussein, M.A., Fahmy, A.R., Fergani, Y.A., Mabrouk, A.M., and Farghaley, S.F., (2015). Toxicological and biochemical studies on use of neonicotinoids and bioinsecticides against the egyptian cotton leaf worm. Spodoptera littoralis (Boisduval) (Lepidoptera: Noctuidae). *Egyptian Journal of Biological Pest Control* 25(3).

[31] Shaurub, El. H., Zohdy, N.Z., Abdel-Aal, A.E., and Emara, S.A., (2018). Effect of chlorfluazuron and flufenoxuron on development and reproductive performance of the black cutworm, Agrotis ipsilon (Hufnagel) (Lepidoptera: Noctuidae). *Invertebrate Reproduction and Development*, *62*(1). https://doi.org/10.1080/07924259.2017.1384407

[32] Abbott, W.S., (1925) A Method of Computing the Effectiveness of an Insecticide. *Journal of Economic Entomology* 18: 265–267, https://doi.org/10.1093/jee/18.2.265a

[33] Finney, D.J., (1971). Probit analysis, 3rd edn. Cambridge University Press, Cambridge, UK

[34] Sun, Y.P., (1950). Toxicity Index-An Improved Method of Comparing the Relative Toxicity of Insecticides1. *Journal of Economic Entomology*, *43*(1). https://doi.org/10.1093/jee/43.1.45

[35] Bradford, M.M., (1976) A rapid and sensitive method for the quantification of microgram quantities of protein utilizing the principle of proteindye binding. Anal Biochem 72: 248–254

[36] Singh, N.B., and Sinha, R.N., (1977). Carbohydrate, Lipid and Protein in the Developmental Stages of Sitophilus oryzae and S. granarius (Coleoptera: Curculionidae) 1. *Annals of the Entomological Society of America* 70: 107-111. https://doi.org/10.1093/aesa/70.1.107

[37] Barnes, H., and Blackstock, J., (1973) Estimation of lipids in marine animals and tissues: Detailed investigation of the sulphophosphovanilun method for “total” lipids. *Journal of Experimental Marine Biology and*

Ecology 12: 103-118. https://doi.org/10.1016/0022-0981(73)90040-3

[38] Ohkawa, H., Ohishi, N., and Yagi, K., (1979). Assay for lipid peroxides in animal tissues by thiobarbituric acid reaction. *Analytical Biochemistry* 95: 351-358. https://doi.org/10.1016/0003-2697(79)90738-3

[39] Beutler, E., Duron, O., and Kelly, B.M., (1963) Improved Method for the Determination of Blood Glutathione. Journal of Laboratory and Clinical Medicine 61: 882-888.

[40] Aebi, H., (1984) Catalase in vitro. In: Renata H (ed) *Methods in Enzymology*, Elsevier, Houston, TX, USA PP 121-126. https://doi.org/10.1016/S0076-6879(84)05016-3

[41] Misra, H.P., and Fridovich, I., (1972). The role of superoxide anion in the autoxidation of epinephrine and a simple assay for superoxide dismutase. *Journal of Biological Chemistry* 247: 3170-3175. https://doi.org/10.1016/s0021-9258(19)45228-9

[42] Asada, K., (1984) [56] Chloroplasts: Formation of Active Oxygen and Its Scavenging. In: Renata H (ed) *Methods in Enzymology*, Elsevier, Houston, TX, USA PP 422-429. https://doi.org/10.1016/S0076-6879(84)05059-X

[43] Simpson, D.R., Bulland, D.L., and Linquist, D,A., (1964). A semi microtechnique for estimation of cholinesterase activity in boll weevils. Annals of the Entomological Society of America 57: 367-371.

[44] Habig, W.H., Pabst, M.J., and Jakoby, W.B., (1974). Glutathione *S*-transferases. J. Biol. Chem. 249: 7130-7139.

[45] Montgomery, H., and Dymock, J.F., (1961). Determination of nitrite in water, royal soc chemistry thomas graham house. *Science Park, Milton Rd, Cambridge* P414.

[46] Hodoroaba, V.D., Motzkus, C., Macé, T., and Vaslin-Reimann, S., (2014). Performance of high-resolution SEM/EDX systems equipped with transmission mode (TSEM) for imaging and measurement of size and size distribution of spherical nanoparticles. *Microscopy and Microanalysis* 20: 602-612. https://doi.org/10.1017/S1431927614000014

[47] Lim, J., Yeap, S.P., Che, H.X., and Low, S.C., (2013). Characterization of magnetic nanoparticle by dynamic light scattering. *Nanoscale Research Letters*, *8*(1). https://doi.org/10.1186/1556-276X-8-381

[48] Chavan, C., Bala, P., Pal, K., and Kale, S.N., (2017) Crosslinked chitosan-dextran sulphate vehicle system for controlled release of ciprofloxaxin drug: An ophthalmic application. *OpenNano*, 2: 28-36. https://doi.org/10.1016/j.onano.2017.04.002

[49] Raval, N., Maheshwari, R., Kalyane, D., Youngren-Ortiz, S.R., Chougule, M.B., and Tekade, R.K., (2018). Importance of physicochemical characterization of nanoparticles. in: Tekade R (ed) pharmaceutical product development. In *Basic Fundamentals of Drug Delivery*, Elsevier, PP 369-400. https://doi.org/10.1016/B978-0-12-817909-3.00010-8

[50] Kaur, I., Goyal, D., and Agnihotri, S., (2021). Formulation of cartap hydrochloride crosslinked chitosan tripolyphosphate nanospheres and its characterization. *Colloid and Polymer Science 299*: 1407-1418. https://doi.org/10.1007/s00396-021-04866-x

[51] Alfy, H., Ghareeb. R.Y., Soltan, E. and Farag, D.A., (2020) Impact of chitosan nanoparticles as insecticide and nematicide against *Spodoptera littoralis*, locusta migratoria, and meloidogyne incognita. *Plant Cell Biotechnology and Molecular Biology* 21: 69–68.

[52] Fahmy, H.M., Abd El-Daim, T.M., Ali, O.A., Hassan, A.A., Mohammed, F.F., and Fathy, M.M., (2021). Surface modifications affect iron oxide nanoparticles' biodistribution after multiple-dose administration in rats. *Journal of Biochemical and Molecular Toxicology* 35(3). https://doi.org/10.1002/jbt.22671

[53] Cai, S., Wu, C., Yang, W., Liang, W., Yu, H. and Liu, L., (2020) Recent advance in surface modification for regulating cell adhesion and behaviors. *Nanotechnology Reviews* 9: 971-989. https://doi.org/10.1515/ntrev-2020-0076

[54] El-Samad, L.M., El-Gerbed, M.S., Hussein, H.S., *et al.*, (2022). Imidacloprid-induced pathophysiological damage in the midgut of Locusta migratoria (Orthoptera: Acrididae) in the field. *Environmental Science and Pollution Research* 29: 57644–57655. https://doi.org/10.1007/s11356-022-19804-9

[55] Li, L., Fang, B., Ren, D., Fu, L., Zhou, Y., Yang, C., Zhang, F., Feng, X., Wang, L., He, X., Qi, P., Liu, Y., Jia, C., Zhao, S., Xu, F., Wei, X. and Wu, H., (2022). Thermal-Switchable, Trifunctional Ceramic-Hydrogel Nanocomposites Enable Full-Lifecycle Security in Practical Battery Systems. *ACS Nano* 16: 10729-10741. https://doi.org/10.1021/acsnano.2c02557

[56] Gao, Z., Pang, L., Feng, H., Wang, S., Wang, Q., Wang, M., Xia, Y., and Hu, S., (2017). Preparation and characterization of a novel imidacloprid microcapsule via coating of polydopamine and polyurea. *RSC Advances* 7: 15762-15768. https://doi.org/10.1039/C7RA01527E

[57] Moradi, F., Hejazi, M.J., Hamishehkar, H., and Enayati, A.A. (2019). Co-encapsulation of

imidacloprid and lambda-cyhalothrin using biocompatible nanocarriers: Characterization and application. *Ecotoxicology and Environmental Safety* 175: 155-163. https://doi.org/10.1016/j.ecoenv.2019.02.092

[58] Nirmala, R., Il, B.W., Navamathavan, R., El-Newehy, M.H., and Kim, H.Y., (2011). Preparation and characterizations of anisotropic chitosan nanofibers via electrospinning. *Macromolecular Research* 19: 345-350. https://doi.org/10.1007/s13233-011-0402-2

[59] Memarizadeh, N., Ghadamyari, M., Adeli, M., and Talebi, K., (2014). Preparation, characterization and efficiency of nanoencapsulated imidacloprid under laboratory conditions. *Ecotoxicology and Environmental Safety* 107: 77-83. https://doi.org/10.1016/j.ecoenv.2014.05.009

[60] Hong, T., Yin, J.Y., Nie, S.P., and Xie, M.Y., (2021). Applications of infrared spectroscopy in polysaccharide structural analysis: Progress, challenge and perspective. *Food Chemistry: X 12*. https://doi.org/10.1016/j.fochx.2021.100168

[61] Al-Syadi, A.M., Faisal, M., Harraz, F.A., Jalalah, M. and Alsaiari, M., (2021) Immersion-plated palladium nanoparticles onto meso-porous silicon layer as novel SERS substrate for sensitive detection of imidacloprid pesticide. *Scientific Reports* 11: 1-14. https://doi.org/10.1038/s41598-021-88326-0

[62] Li, Z., Li, M., He, J., Zhao, X., Chaimanee, V., Huang, W., Nie, H., Zhao, Y., and Su, S., (2017). Differential physiological effects of neonicotinoid insecticides on honey bees: A comparison between *Apis mellifera* and *Apis cerana*. Pestic. Biochem. Physiol. 140: 1-8. https://doi.org/10.1016/j.pestbp.2017.06.010

[63] Elsayed, A., Al-Remawi, M., Maghrabi, I., Hamaidi, M., and Jaber, N., (2014). Development of insulin loaded mesoporous silica injectable particles layered by chitosan as a controlled release delivery system. *International Journal of Pharmaceutics* 461: 448-458. https://doi.org/10.1016/j.ijpharm.2013.12.014

[64] Qian, K., Guo, Y., and He, L., (2012). Controlled release of imidacloprid from poly (styrene-diacetone crylamide)-based nanoformulation. *International Journal of Nanoscience*, *11*(6). https://doi.org/10.1142/S0219581X12400364

[65] Lei, Z., and Bi, S., (2007). The silica-coated chitosan particle from a layer-by-layer approach for pectinase immobilization. *Enzyme and Microbial Technology* 40: 1442-1447. https://doi.org/10.1016/j.enzmictec.2006.10.027

[66] Sabbour, M.M., (2015). Nano-Imidaclorprid against three olive pests under laboratory and field conditions. J. Biosci. Bioengin 2: 45-49.

[67] Sabbour, M.M., and Shaurub, E.S.H., (2018). Toxicity effect of Imidacloprid and nano-Imidacloprid particles in controlling Bactrocera oleae (Rossi) (Diptera: Tephritidae) under laboratory and field conditions. *Bioscience Research* 15: 2494:2501.

[68] El-Saleh, M., El-Sheikh, E., Aioub, A., and Desuky, W., (2016). Biochemical changes in a field strain of *Spodoptera littoralis* (boisd.) (lepidoptera: noctuidae) after exposure to the field rates of neonicotinoid insecticides in artificial diet. *Zagazig Journal of Agricultural Research 43*: 225-234. https://doi.org/10.21608/zjar.2016.101881

[69] Nath, B.S., Suresh, A., Varma, B.M. and Kumar, R.P. (1997). Changes in protein metabolism in hemolymph and fat body of the silkworm, Bombyx mori (Lepidoptera: Bombycidae) in response to organophosphorus insecticides toxicity. *Ecotoxicology and environmental safety* 36: 169–173. https://doi.org/10.1006/eesa.1996.1504

[70] Canavoso, L.E., Jouni, Z.E., Karans, K.J., Pennington, J.E., and Wells, M.A., (2001). Fat metabolism in insects. Annu. Rev. Nutr. 21: 23-46.

[71] Remia, K.M., Logaswamy, K., and Rajmohan, D., (2008). Effect of an insecticide (Monocrotophos) on some biochemical constituents of the fish *Tilapia mossambica*. Pollut. Res. 27: 523-526.

[72] Li-Byarlay, H., and Cleare, X.L., (2020). Current trends in the oxidative stress and ageing of social hymenopterans. Adv. Insect Physiol 59: 43-69. https://doi.org/10.1016/bs.aiip.2020.09.002

[73] Zhan, E.L., Wang, Y., Jiang, J., Jia, Z.Q., Tang, T., Song, Z.J., Han, Z.J., and Zhao, C.Q., (2021). Influence of three insecticides targeting GABA receptor on fall armyworm *Spodoptera frugiperda*: Analyses from individual, biochemical and molecular levels. Pestic. Biochem. Physiol 179: 1-7. https://doi.org/10.1016/j.pestbp.2021.104973

[74] Balieira, K.V.B., Mazzo, M., Bizerra, P.F.V., Guimaraes, A.R.J.S., Nicodemo, D., and Mingatto, F.E., (2018) Imidacloprid-induced oxidative stress in honey bees and the antioxidant action of caffeine. Apidologie 49: 562-572. https://doi.org/10.1007/s13592-018-0583-1

[75] Vijayavel, K., and Balasubramanian, M.P., (2009). Effect of fenvalerate on oxidative stress biomarkers in the brackish water prawn Penaeus monodon. *Pesticide Biochemistry and Physiology* 95: 113-116. https://doi.org/10.1016/j.pestbp.2009.07.011.

[76] Rojas, R.R., and Leopold, R.A., (1996). Chilling injury in the housefly: Evidence for the role of

oxidative stress between pupariation and emergence. *Cryobiology* 33: 447-458. https://doi.org/10.1006/cryo.1996.0045

[77] Vethanayagam, J.G., Green, E.H., Rose, R.C., and Bode, A.M., (1999). Glutathione-dependent ascorbate recycling activity of rat serum albumin. *Free radical biology & medicine* 26: 1591–1598. https://doi.org/10.1016/s0891-5849(99)00031-3

[78] Alin, P., Danielson, U.H., and Mannervik, B., (1985) 4-Hydroxyalk-2-enals are substrates for glutathione transferase. *FEBS letters* 179: 267–270. https://doi.org/10.1016/0014-5793(85)80532-9

[79] Kumar, M.R., Reddy, A.G., Anjaneyulu, Y., and Reddy, G.D., (2010). Oxidative stress induced by lead and antioxidant potential of certain adaptogens in poultry. *Toxicology International* 17: 45-48. https://doi.org/10.4103/0971-6580.72668

[80] Ezeji, E.U., Anyalogbu, E.A., Ezejiofor, T.N., and Udensi, J.U., (2012). Determination of Reduced Glutathione and Glutathione S-transferase of Poultry Birds Exposed to Permethrin Insecticide. *American Journal of Biochemistry* 2: 21-24. https://doi.org/10.5923/j.ajb.20120203.01

[81] Yousef, H.A., Abdelfattah, E.A., and Augustyniak, M., (2017). Evaluation of oxidative stress biomarkers in Aiolopus thalassinus (Orthoptera: Acrididae) collected from areas polluted by the fertilizer industry. *Ecotoxicology* 26: 340-350. https://doi.org/10.1007/s10646-017-1767-6

[82] Halliwell, B., and Gutteridge, J.M.C., (2015). *Free Radicals in Biology and Medicine*, 5th edn, Oxford. https://doi.org/10.1093/acprof:oso/9780198717478.001.0001

[83] Dutta, P., Dey, T., Manna, P., and Kalita, J., (2016). Antioxidant potential of Vespa affinis L., a traditional edible insect species of North East India. PLoS One 11(5):e0156107. https://doi:10.1371/journal.pone.0156107

[84] Conners, D.E., (2004). Biomarkers of oxidative stress in freshwater clams (Corbicula fluminea) as mechanistic tools to evaluate the impairment of stream ecosystem health by lawn care pesticides. University of Georgia. https://api.semanticscholar.org/CorpusID:91169802

[85] Chakrabarti, P., Rana, S., Sarkar, S., Smith, B., and Basu, P., (2015) Pesticide-induced oxidative stress in laboratory and field populations of native honey bees along intensive agricultural landscapes in two Eastern Indian states. *Apidologie*, 46: 107-129. https://doi.org/10.1007/s13592-014-0308-z

[86] Sofo, A., Scopa, A., Nuzzaci, M., and Vitti, A., (2015). Review. Ascorbate peroxidase and catalase activities and their genetic regulation in plants subjected to drought and salinity stresses. Int J Mol Sci 16: 13561–13578. http://doi:10.3390/ijms160613561

[87] Huang, Y., Xu, Z., Lin, X., Feng, Q., and Zheng, S., (2011). Structure and expression of glutathione S-transferase genes from the midgut of the Common cutworm, Spodoptera litura (Noctuidae) and their response to xenobiotic compounds and bacteria. *Journal of insect physiology* 57: 1033–1044. https://doi.org/10.1016/j.jinsphys.2011.05.001

[88] Sheehan, D., Meade, G., Foley, V.M., and Dowd, C.A., (2001). Structure, function and evolution of glutathione transferases: implications for classification of non-mammalian members of an ancient enzyme superfamily. *The Biochemical journal* 360: 1–16. https://doi.org/10.1042/0264-6021:3600001

[89] Delkash-Roudsari, S., Goldansaz, S.H., Talebi Jahromi, K., Ashouri, A., and Abramson, C.I., (2022). Side effects of imidacloprid, ethion, and hexaflumuron on adult and larvae of honey bee Apis mellifera (Hymenoptera, Apidae). *Apidologie* 53(1). https://doi.org/10.1007/s13592-022-00910-z

[90] Lu, W., Liu, Z., Fan, X., Zhang, X., Qiao, X., and Huang, J., (2022). Nicotinic acetylcholine receptor modulator insecticides act on diverse receptor subtypes with distinct subunit compositions. *PLoS Genetics 18*(1). https://doi.org/10.1371/journal.pgen.1009920

[91] Watson, G.B., Chouinard, S.W., Cook, K.R., Geng, C., Gifford, J.M., Gustafson, G.D., Hasler, J.M., Larrinua, I.M., Letherer, T.J., Mitchell, J.C., Pak, W.L., Salgado, V.L., Sparks, T.C., and Stilwell, G.E., (2010). A spinosyn-sensitive Drosophila melanogaster nicotinic acetylcholine receptor identified through chemically induced target site resistance, resistance gene identification, and heterologous expression. *Insect Biochemistry and Molecular Biology* 40: 376-384. https://doi.org/10.1016/j.ibmb.2009.11.004

[92] Sule, R.O., Condon, L., and Gomes, A.v.,(2022). A Common Feature of Pesticides: Oxidative Stress - The Role of Oxidative Stress in Pesticide-Induced Toxicity. In *Oxidative Medicine and Cellular Longevity* (Vol. 2022). https://doi.org/10.1155/2022/5563759

[93] Alhasawi, A., Jagadeesan, S., Appanna, V., Appanna, V., and Legendre, F., (2019) Biochemical Strategies to Counter Nitrosative Stress. In: Das S and Dash H *Microbial Diversity in the Genomic Era*, 1st edn. Elsevier, PP153-169

https://doi.org/10.1016/B978-0-12-814849-5.00010-1

[94] Martínez, M.C., and Andriantsitohaina, R., (2009). Reactive nitrogen species: Molecular mechanisms and potential significance in health and disease. In *Antioxidants and Redox Signaling* 11(3). https://doi.org/10.1089/ars.2007.1993

[95] Li, Y.R. and Trush, M., (2016). Defining ROS in Biology and Medicine. *Reactive Oxygen Species* 1: 9-21. https://doi.org/10.20455/ros.2016.803

[96] Dorrah, M.A., Mohamed, A.A., and Shaurub, E.S.H., (2019). Immunosuppressive effects of the limonoid azadirachtin, insights on a nongenotoxic stress botanical, in flesh flies. *Pesticide Biochemistry and Physiology* 153: 55-66. https://doi.org/10.1016/j.pestbp.2018.11.004

[97] Wink, D.A., and Mitchell, J.B., (1998). Chemical biology of nitric oxide: Insights into regulatory, cytotoxic, and cytoprotective mechanisms of nitric oxide. *Free Radical Biology and Medicine* 25: 434-456. https://doi.org/10.1016/S0891-5849(98)00092-6

[98] Rivero, A., (2006). Nitric oxide: an antiparasitic molecule of invertebrates. In *Trends in Parasitology* 22: 219-225. https://doi.org/10.1016/j.pt.2006.02.014